AD-A120 421 DIGITAL REDESIGN OF EXISTING MULTILOOP CONTINUOUS CONTROL SYSTEMS VIA CON..(U) WRIGHT STATE UNIV DAYTON OHIO DEPT OF ENGINEERING K S RATTAN SEP 82 1/1

UNCLASSIFIED AFOSR-TR-82-0915 AFOSR-81-0132 F/G 9/2 NL

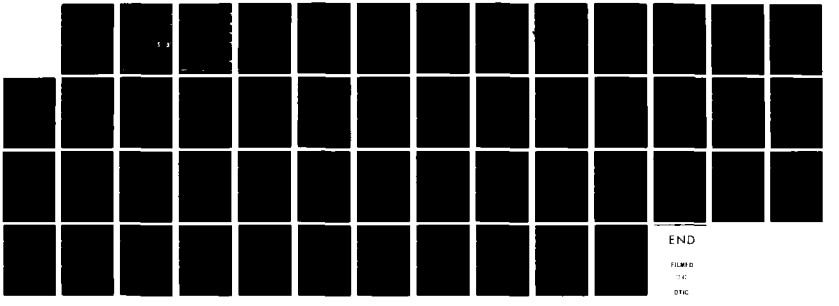

END

FILMED

DTIC

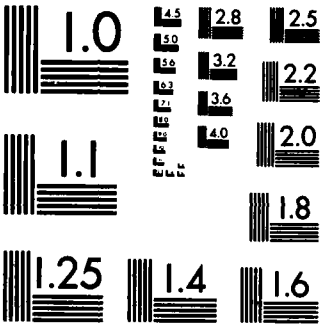

REPORT DOCUMENTATION PAGE		READ INSTRUCTIONS BEFORE COMPLETING FORM
1. REPORT NUMBER AFOSR-TR- 82-0915	2. GOVT ACCESSION NO. AD-A120421	3. RECIPIENT'S CATALOG NUMBER
4. TITLE (and Subtitle) DIGITAL REDESIGN OF EXISTING MULTILOOP CONTINUOUS CONTROL SYSTEMS VIA CONTINUOUS FREQUENCY MATCHING [redacted]		5. TYPE OF REPORT & PERIOD COVERED FINAL, 1 MAY 81-1 JUN 82 6. PERFORMING ORG. REPORT NUMBER
7. AUTHOR(s) Kuldip S. Rattan		8. CONTRACT OR GRANT NUMBER(s) AFOSR-81-0132
9. PERFORMING ORGANIZATION NAME AND ADDRESS Department of Engineering Wright State University Dayton OH 45435		10. PROGRAM ELEMENT, PROJECT, TASK AREA & WORK UNIT NUMBERS PE61102F; 2304/A4
11. CONTROLLING OFFICE NAME AND ADDRESS Directorate of Mathematical & Information Sciences Air Force Office of Scientific Research Bolling AFB DC 20332		12. REPORT DATE September 1982 13. NUMBER OF PAGES 51
14. MONITORING AGENCY NAME & ADDRESS(if different from Controlling Office)		15. SECURITY CLASS. (of this report) UNCLASSIFIED 15a. DECLASSIFICATION/DOWNGRADING SCHEDULE

16. DISTRIBUTION STATEMENT (of this Report)
Approved for public release; distribution unlimited.

17. DISTRIBUTION STATEMENT (of the abstract entered in Block 20, if different from Report)

DTIC ELECTE OCT 19 1982 S D F

18. SUPPLEMENTARY NOTES

19. KEY WORDS (Continue on reverse side if necessary and identify by block number)
Digital control; computer-aided design; digitalization of existing continuous systems.

20. ABSTRACT (Continue on reverse side if necessary and identify by block number)
The problem of converting existing multiloop continuous control systems into digital control systems is considered. The objective of this paper is to develop a computer-aided method for synthesizing the pulse-transfer function of the digital controllers. This is done by matching the continuous frequency responses of the digital control system to those of a continuous system with a minimum weighted mean square error. Formulas for computing the parameters of digital controllers are obtained as a result. An example of digitalizing the existing continuous flight controller for the longitudinal YF-16 aircraft (CONTINUED)

DD FORM 1 JAN 73 1473

UNCLASSIFIED
SECURITY CLASSIFICATION OF THIS PAGE (When Data Entered)

ITEM #20, CONTINUED: is considered and the results are compared with those obtained by previous methods.

TABLE OF CONTENTS

LIST OF ILLUSTRATIONS

SECTION I

INTRODUCTION

Digital controls are the subject of expanding interest in both the academic and industrial communities. This is especially true since the advent of the economical microprocessor and its related support chips which have made digital control an attractive alternative when considering a control strategy. For the past few years new control systems have been designed using digital instead of analog controllers. There is also a need for converting systems which were designed to be controlled by continuous controllers into systems to be controlled by digital controllers. Conversion of existing control systems is a problem of considerable interest to various branches of industry.

A popular method for converting existing control systems into digital control systems is by Tabak.[1] This method converts the transfer function of the continuous controller into a pulse-transfer function of the digital controller using prewarped bilinear transformation. The method is straightforward and easy to use, but the digital control system obtained by this method approximates the continuous control system only when the sampling frequency is sufficiently high as compared with the highest frequency of the continuous system. This is because the tranfer function of the plant and the feedback element are not taken into consideration. Thus the capabilities of the digital controller are not fully utilized.

Kuo et al.,[2] Yackel et al.[3] and Singh et al.[4] in their papers proposed methods for converting a continuous control system into a sampled-data control system by matching the unit-step response of the systems at all sampling instants or at multiples of sampling instants. The matching requirements are satisfied by changing the input and feedback gains of the system instead of using a digital controller. However, such matching holds only for unit step input. Thus the performance of the sampled-data system obtained by their method approximates that of the continuous system only when the input frequency is sufficiently low in comparison with the sampling frequency. For higher input frequencies, the approximation is poor.

Recently the author of this report and Yeh[5] proposed a computer-aided method for converting an existing continuous control system into a digital control system by matching the discrete frequency response of the discretly excited system to the frequency response of the continuous model with a minimum weighted mean square error. The discrete frequency response of the digital control system was obtained by inserting an artificial sampler of duration T at the output of the system and then substituting $z = e^{j\omega T}$ in the overall pulse-transfer function of the system. Even though the results obtained by this method were superior to the ones obtained by Tabak's[1] and other methods, this method only matched the response of the systems at the sampling instants. The purpose of this study is to improve on this method by matching the continuous frequency response of the discretly excited system to that of the continuous model. The synthesis of the digital controller is carried out by minimizing an error between the continuous frequency response of the digital and existing systems in the w-domain. The method uses the complex curve fitting technique of Levy.[6] As a result the formulas for computing the parameters of the digital controller are obtained. This method is then extended to the digital redesign of an existing multiloop continuous control system. The design algorithms developed here are based on the transfer function of the plant and the closed-loop transfer function of different loops of the continuous system. As a particular application, the digitalization of a flight control system is discussed. The system under consideration is the flight controller for the longitudinal YF-16 aircraft. The results obtained by this method are compared with those obtained by the previous methods.

SECTION II

STATEMENT OF THE PROBLEM

The block diagram of a general multiloop continuous-data control system may be drawn as shown in Figure 1

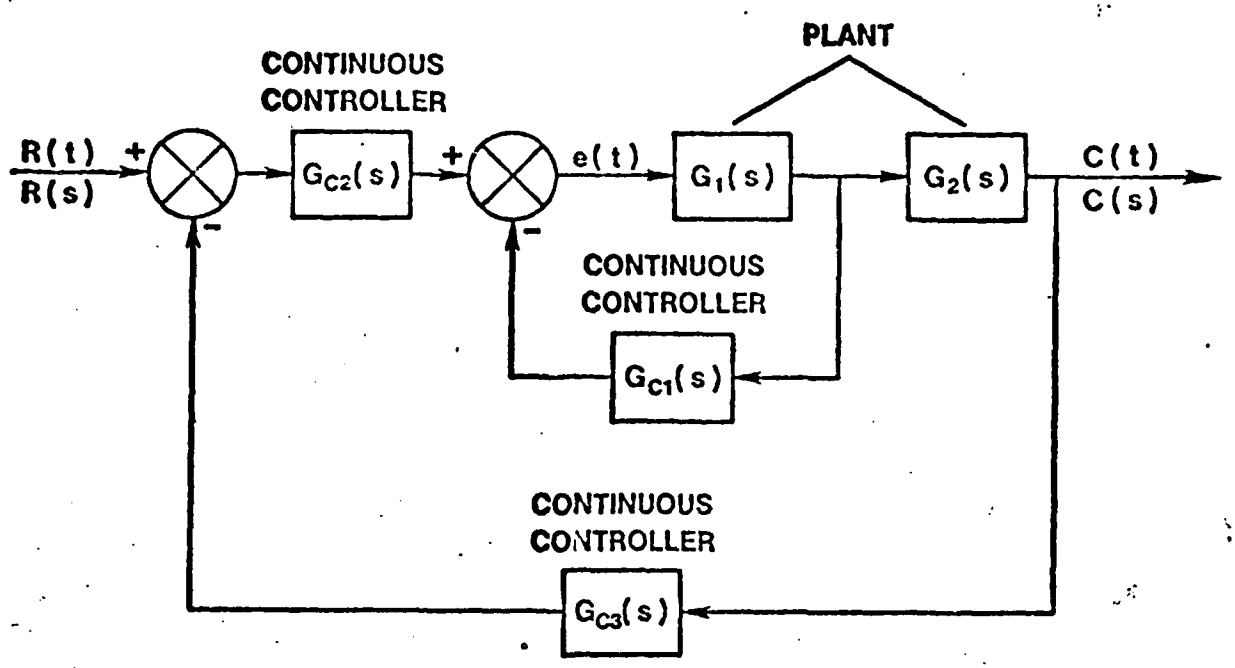

Figure 1. Existing multiloop continuous-data control system

The continuous model shown in Figure 1 can be digitalized by inserting a sampler at the error input e(t) and replacing the continuous compensators $G_{ci}(s)$ by digital controller $D_i(z)$ as shown in Figure 2.

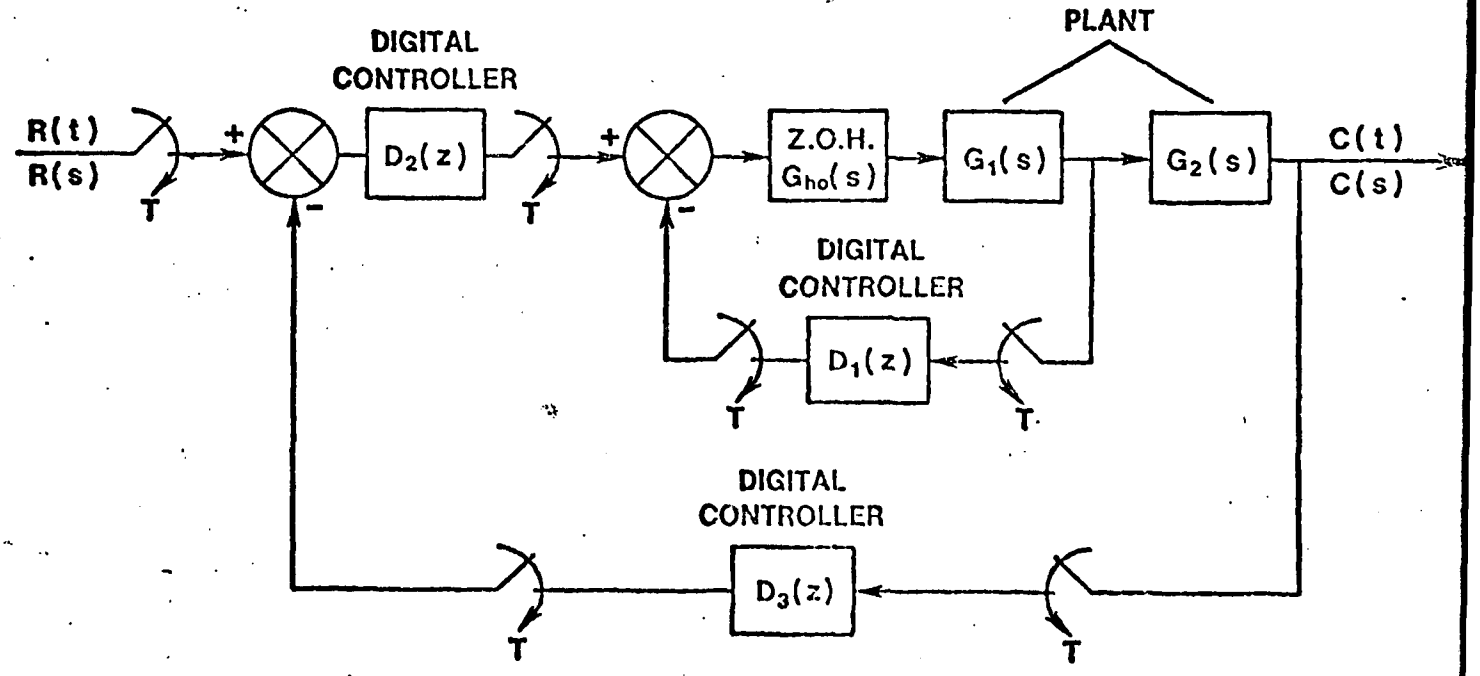

Figure 2. Multiloop digital control system

The general pulse-transfer function of a digital controller may be written as

$$D(z) = \frac{c_0+c_1z^{-1}+c_2z^{-2}+\cdots+c_mz^{-m}}{1+d_1z^{-1}+d_2z^{-2}+\cdots+d_nz^{-n}} \quad , \; m\leq n \tag{1}$$

where a's and b's are unknown constants. It is required to design digital controllers, i.e., to find the unknown constants of different controllers so that the steady state output of the digital control system follows the desired output of the continuous model for all sinusoidal inputs within the frequency range. This is done by matching the continuous frequency responses of different loops of the digital control system to the corresponding ideal frequency responses starting from the innermost loop.

SECTION III

DESIGN OF DIGITAL CONTROLLERS VIA CONTINUOUS FREQUENCY MATCHING

1. Digital Controller in the Feedback Loop

The block diagram of the inner loop of the digital control system shown in Fig. 2 is redrawn as shown in Figure 3.

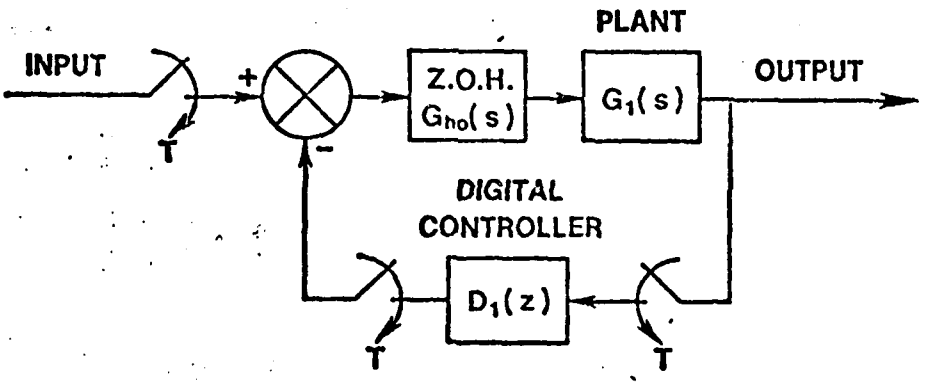

Figure 3. Inner loop of digital control system shown in Figure 2

The overall transfer function of the continuous and digital systems (inner loop) can be written from Figures 1 and 3 respectively as

$$\frac{C_{m1}(s)}{R_1(s)} = F_1(s) = \frac{G_1(s)}{1+G_1(s)G_{c1}(s)} \tag{2}$$

$$\frac{C_{d1}(s)}{R_1^T(s)} = G_{d1}(s) = \frac{G_{h0}G_1(s)}{1+D_1^T(s)\overline{G_{h0}G_1}^T(s)} \tag{3}$$

where $G_{c1}(s)$, $G_{h0}(s)$ and $G_1(s)$ are the transfer functions of the continuous controller, zero-order hold and plant respectively. The superscript notation denotes the sampling rate. For example R_1^T indicates that the signal R_1 is sampled at $\frac{1}{T}$ samples/second.

It is required to design a digital controller, $D_1(z)$, by matching the continuous frequency response of the digital control system shown in Figure 3 to the corresponding ideal frequency response of the continuous model shown in Figure 1. The frequency response of the continuous model can be obtained by substituting $s = j\omega$ in equation (2) and varying ω from 0 to ∞. But because of the hybrid nature of equation (3), a common way of finding the frequency response of the digital control system is to put an artificial sampler of duration T seconds at the output of the system, substituting $z = e^{j\omega T}$ in the overall z-transfer function and then varying ω from 0 to π/T. We will call this discrete frequency response. Recently the Author[7] proposed a method for converting an existing multiloop continuous control system into a digital control system by matching the discrete frequency responses of the digital control system to the frequency responses of the continuous model. In this method we only matched the response at the sampling instants. It is this observation which prompted the development of the method in this report which matches the continuous frequency responses of the discretly excited system shown in Figure 1 to those of the continuous system shown in Figure 2. Rewriting equation (3) with $z = e^{st}$, we get

$$G_{d1}(s) = \frac{G_{h0}G_1(s)}{1+D_1(z)\overline{G_{h0}G_1}(z)} \tag{4}$$

where

$$\overline{G_{h0}G_1}(z) = z[G_{h0}G_1(s)] \tag{5}$$

Then, the continuous frequency response of this discretly excited system is given by (Didaleusky and Whitback[8])

$$A_n+jB_n = \frac{1}{T} G_{h0}G_1(s)\Big|_{s=j\omega_n} \frac{1}{1+D(z)\overline{G_{h0}G_1}(z)}\Bigg|_{z = 1 \angle bT}^{z \triangleq e^{sT}} \tag{6}$$

where

$$\omega_n = b + \frac{2\pi n}{T} \quad , \quad n = 0,1,2,3, \cdots \tag{7}$$

For n=0, we get the fundamental component of the output response (i.e. $C_{d1}(s)$ for a sampled sinusoidal input R(z)). For $n\neq 0$, we get the output response for the individual alias frequency components. For example, for n=1

$$\omega_1 = b + \frac{2\pi}{T} = b + \omega_s \tag{8}$$

and we get the frequency response in the output for the 1st alias component.

At this point it is important to recognize that the actual continuous response, $C_{d1}(s)$, is not sinusoidal. This becomes clear in the time domain response for $C_{d1}(s)$ for a sampled input $R_1(z)$ (Whitback and Hoffman[9]). It is apparant that the best we can do is match the fundamental component of the output response $C_{d1}(s)$. An alternate w-domain expression for equation (6) is given by

$$A_n+jB_n = \frac{1}{T} G_{h0}G_1(s)\Big|_{s=j\omega_n} G_A(w)\Big|_{w=j\frac{2}{T}\tan\frac{\omega_n T}{2}} \tag{9}$$

where

$$G_A(w) = \frac{1}{1+D(z)\overline{G_{h0}G_1}(z)}\Bigg|_{z=\frac{1+\frac{wT}{2}}{1-\frac{wT}{2}}} \tag{10}$$

Equations (6) and (9) provide the same continuous frequency response of the discretely excited system but the advantage of using equation (9) is that it improves numerical round off problem in the implementation algorithms. Equation (9) can be written as

$$G_{d1}(w) = \frac{w}{1+\frac{wT}{2}} \frac{1}{1+D(z)\overline{G_{h0}G_1}(z)} \left| \frac{G_1(s)}{s} \right|_{z=\frac{1+\frac{wT}{2}}{1-\frac{wT}{2}}} \Bigg|_{s=j\frac{2}{T}\tan^{-1}\frac{wT}{2j}} \tag{11}$$

Let the transfer function of the digital controller, D_1, be written in the w-domain as

$$D_1(w) = \frac{a_{1,m}w^m + a_{1,m-1}w^{m-1} + \cdots\cdots + a_{1,1}w + a_{1,0}}{b_{1,n}w^n + b_{1,n-1}w^{n-1} + \cdots\cdots + b_{1,1}w + 1} \tag{12}$$

where $a_{1,i}$'s and $b_{1,i}$'s are constants to be determined. The continuous frequency responses of the digital and continuous system can now be obtained by substituting $w = j\gamma$ and $s = j\frac{2}{T}\tan^{-1}\frac{\gamma T}{2}$ in equations (11) and (2) respectively

$$F_1(j\gamma) = F_1(s)\Big|_{s=j\frac{2}{T}\tan^{-1}\frac{\gamma T}{2}} = A_1 + jB_1 \tag{13}$$

$$G_{d1}(j\gamma) = \frac{(X_{11}+jY_{11})}{1+\frac{P_1+j\gamma Q_1}{1+L_1+j\gamma M_1}(X_{21}+jY_{21})} \tag{14}$$

where

$$P_1 = a_{1,0} - a_{1,2}\gamma^2 + a_{1,4}\gamma^4 - a_{1,6}\gamma^6 + \cdots \tag{15}$$

$$Q_1 = a_{1,0} - a_{1,3}\gamma^2 + a_{1,5}\gamma^4 - a_{1,7}\gamma^6 + \cdots \tag{16}$$

$$L_1 = 0 - b_{1,2}\gamma^2 + b_{1,4}\gamma^4 - b_{1,6}\gamma^6 + \cdots\cdots \tag{17}$$

$$M_1 = b_{1,1} - b_{1,3}\gamma^2 + b_{1,5}\gamma^4 - b_{1,7}\gamma^6 + \cdots \tag{18}$$

$$X_{11}+jY_{11} = \frac{j\gamma}{1+j\frac{\gamma T}{2}} \frac{G_1(s)}{s}\Bigg|_{s=j\frac{2}{T}\tan^{-1}\frac{\gamma T}{2}} \tag{19}$$

$$X_{21}+jY_{21} = \overline{G_{h0}G_1}(z)\Big|_{z=\frac{1+j\gamma\frac{T}{2}}{1-j\gamma\frac{T}{2}}} \tag{20}$$

For notation convenience, let the numerator and denominator of $G_{d1}(j\gamma)$ be denoted by $N(\gamma)$ and $M(\gamma)$ respectively, i.e.

$$G_{d1}(j\gamma) = \frac{N(\gamma)}{M(\gamma)} \tag{21}$$

In terms of real and imaginary parts, $N(\gamma)$ and $M(\gamma)$ can be written as

$$N(\gamma) = \phi+j\theta \tag{22}$$

$$M(\gamma) = \sigma+j\tau \tag{23}$$

where

$$\phi = (1+L_1)X_{11}-\gamma M_1 Y_{11} \tag{24}$$

$$\theta = (1+L_1)Y_{11}+\gamma M_1 X_{11} \tag{25}$$

$$\sigma = 1+L_1+P_1X_{21}-\gamma Q_1 Y_{21} \tag{26}$$

$$\tau = \gamma M_1+P_1Y_{21}+\gamma Q_1 X_{21} \tag{27}$$

The error between $G_{d1}(j\gamma)$ and $F_1(j\gamma)$ is defined as

$$\varepsilon(\gamma) = F_1(j\gamma)-G_{d1}(j\gamma) \tag{28}$$

An optimal set of a's and b's can therefore be optained by minimizing the mean square of the magnitude of $\varepsilon(\gamma)$ Let the error function to be minimized be defined as

$$E = \int_{\gamma_1}^{\gamma_2} \left| F_1(j\gamma) - \frac{N(\gamma)}{M(\gamma)} \right|^2 d\gamma \tag{29}$$

where $(\gamma_2-\gamma_1)$ is the bandwidth in the w-dom 'n on which the matching is required This error function is to be minimized by adjusting the unknown coefficients $a_{1,i}$ and $b_{1,i}$. However, due to the presence of $M(\gamma)$ in the denominator, the equations obtained by differentiating E with respect to $a_{1,i}$ and $b_{1,i}$ are nonlinear. This nonlinearity may be removed by modifying the error function (29) as

$$E_{ml} = \int_{\gamma_1}^{\gamma_2} \left| F_1(j\gamma)M(\gamma) - N(\gamma) \right|^2 d\gamma \tag{30}$$

This integral differs from that in equation (29) by including $|M(\gamma)|^2$ in the integrand as a weighting factor. This modification is not new. It was suggested by Kalman[10] as an identification technique, was used by Levy [6] in complex curve fitting, Rao and Lamba[11] for simplifying linear systems and by the author and Yeh[5] for discretizing continuous systems.

The integrand in equation (3) is a complex function and may be seperated into real and imaginary part as

$$\left| F_1(j\gamma)M(\gamma) - N(\gamma) \right| = \ell(\gamma) + jm(\gamma) \tag{31}$$

where

$$\ell(\gamma) = A_1\sigma - B_1\tau - \phi \tag{32}$$

$$m(\gamma) = A_1\tau + B_1\sigma - \theta \tag{33}$$

By substituting equations (31)-(33) in (30), we get

$$E_{ml} = \int_{\gamma_1}^{\gamma_2} \left[(A_1\sigma - B_1\tau - \phi)^2 + (A_1\tau + B_1\sigma - \theta)^2 \right] d\gamma \tag{34}$$

Differentiating E_{ml} with respect to $a_{l,i}$'s and $b_{l,i}$'s and equating the resulting equations to zero represents (m+n+1) linear equations in (m+n+1) unknowns $a_{l,0}$ to $a_{l,m}$ and $b_{l,l}$ to $b_{l,n}$. These equations can be written in the matrix form as given in equation (35)

$$\begin{bmatrix} a_{l,o} \\ a_{l,1} \\ a_{l,2} \\ a_{l,3} \\ \vdots \\ b_{l,1} \\ b_{l,2} \\ b_{l,3} \\ b_{l,4} \\ \vdots \end{bmatrix} = \begin{bmatrix} T_o & 0 & -T_2 & 0 & T_4 & 0 \cdots & V_1 & -U_2 & -V_3 & U_4 & V_5 & -U_6 & \cdots \\ 0 & T_2 & 0 & -T_4 & 0 & T_6 \cdots & U_2 & V_3 & -U_4 & -V_5 & U_6 & -V_7 & \cdots \\ -T_2 & 0 & T_4 & 0 & -T_6 & 0 \cdots & -V_3 & U_4 & V_5 & -U_6 & -V_7 & U_8 & \cdots \\ 0 & -T_4 & 0 & T_6 & 0 & -T_8 \cdots & -U_4 & -V_5 & U_6 & V_7 & -U_8 & -V_8 & \cdots \\ \vdots & & & & & & & & & & & & \\ V_1 & U_2 & -V_3 & -U_4 & V_5 & U_6 \cdots & W_2 & 0 & -W_4 & 0 & W_6 & 0 & \cdots \\ -U_2 & V_3 & U_4 & -V_5 & -U_6 & V_7 \cdots & 0 & W_4 & 0 & -W_6 & 0 & W_8 & \cdots \\ -V_3 & -U_4 & V_5 & U_6 & -V_7 & -U_8 \cdots & -W_4 & 0 & W_6 & 0 & -W_8 & 0 & \cdots \\ U_4 & -V_5 & -U_6 & V_7 & U_8 & -V_9 \cdots & 0 & W_6 & 0 & W_8 & 0 & -W_{10} & \cdots \\ \vdots & & & & & & & & & & & & \end{bmatrix}^{-1} \begin{bmatrix} -U_o \\ V_1 \\ U_2 \\ -V_3 \\ \vdots \\ 0 \\ W_2 \\ 0 \\ W_4 \\ \vdots \end{bmatrix} \tag{35}$$

where

$$T_h = \int_{\gamma_1}^{\gamma_2} \left(A_1^2+B_1^2\right)\left(X_{21}^2+Y_{21}^2\right)\gamma^h d\gamma \tag{36}$$

$$U_h = \int_{\gamma}^{\gamma_2} \left[\left(A_1^2+B_1^2\right)X_{21} - A_1\left(X_{11}X_{21}+Y_{11}Y_{21}\right)+B_1\left(X_{11}Y_{21}-X_{21}Y_{11}\right)\right]\gamma^h d\gamma \tag{37}$$

$$V_h = \int_{\gamma_1}^{\gamma_2} \left[\left(A_1^2+B_1^2\right)Y_{21} - A_1\left(X_{11}Y_{21}-X_{21}Y_{11}\right)-B_1\left(X_{11}X_{21}+Y_{11}Y_{21}\right)\right]\gamma^h d\gamma \tag{38}$$

$$W_h = \int_{\gamma_1}^{\gamma_2} \left[\left(A_1^2+B_1^2\right)+\left(X_{11}^2+Y_{11}^2\right)-2\left(A_1X_{11}+B_1Y_{11}\right)\right]\gamma^h d\gamma \tag{39}$$

Equations (35)-(39) provide a design algorithm which has been programmed on a digital computer (IBM 370/3031) and is available in the form of a subroutine written in FORTRAN IV. Note that the order of the digital controller (integer m and n) is arbitrary. Therefore, using this algorithm, one may try out several digital controllers of different orders and select the best design by considering the tradeoff between cost (complexity) and performance. The pulse-transfer function of the digital controller D_1 can now be obtained as

$$D_1(z) = D_1(w)\Big|_{w = \frac{2}{T}\frac{z-1}{z+1}} \tag{40}$$

2. Digital Controller, $D_2(z)$, in the Feedforward path of Outer Loop

The block diagram shown in Figure 4 is obtained from Figure 1 after inserting a sampler at the error input e(t), replacing continuous compenstor $G_{c1}(s)$ by the already designed controller $D_1(z)$ and replacing the controller $G_{c2}(s)$ by the yet to be designed digital controller $D_2(z)$.

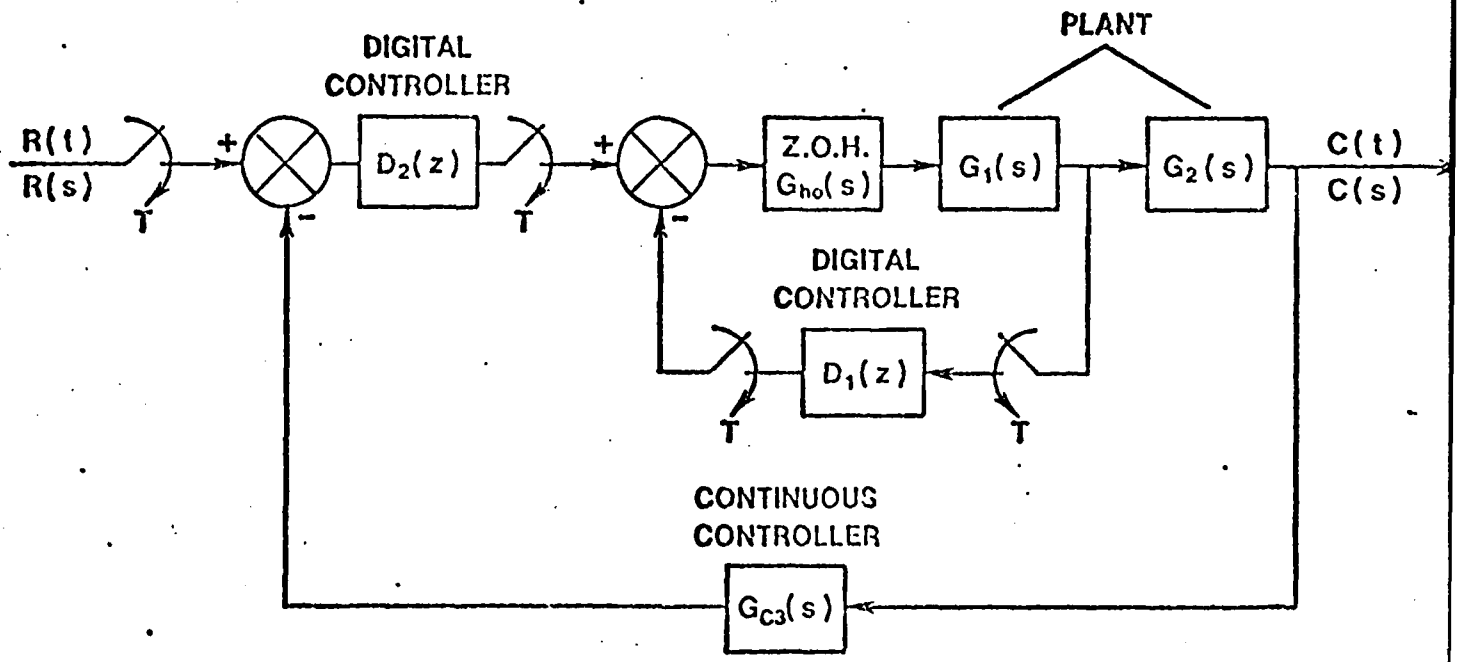

Figure 4. Digital control system with unknown digital controller in the feedforward outer loop.

The overall transfer functions (outer loop) of the digital control system as shown in Figure 4 and the continuous control system shown in Figure 1 can be written in w-domain as

$$F_2(w) = \left. \frac{G_{c2}(s)F_1(s)G_2(s)}{1+G_{c3}(s)G_{c2}(s)F_1(s)G_2(s)} \right|_{s=j\frac{2}{T}\tan^{-1}\frac{wT}{2j}} \tag{41}$$

$$G_{d2}(w) = \frac{w}{1+\frac{wT}{2}} \left. \frac{D_2(z)\,\dfrac{1}{1+\overline{G_{h0}G_1}(z)D_1(z)}}{1+D_2(z)\,\dfrac{\overline{G_{h0}G_1G_2G_{c3}}(z)}{1+\overline{G_{h0}G_1}(z)D_1(z)}} \right|_{z=\frac{1+\frac{wT}{2}}{1-\frac{wT}{2}}} \left. \frac{G_1G_2(s)}{s} \right|_{s=j\frac{2}{T}\tan^{-1}\frac{wT}{2j}} \tag{42}$$

where

$$\overline{G_{h0}G_1G_2}(z) = z\left[G_{h0}G_1G_2(s)\right] \tag{43}$$

$$\overline{G_{h0}G_1G_2G_{c3}}(z) = z\left[G_{h0}G_1G_2G_{c3}(s)\right] \tag{44}$$

Let the transfer function of the digital controller, $D_2(w)$, be written in the w-domain as

$$D_2(w) = \frac{a_{2,m}w^m + a_{2,m-1}w^{m-1} + \cdots\cdots + a_{2,1}w + a_{2,0}}{b_{2,n}w^n + b_{2,n-1}w^{n-1} + \cdots\cdots + b_{2,1}w + 1}, \quad m \leq n \tag{45}$$

where $a_{2,i}$'s and $b_{2,i}$'s are constants to be determined. The continuous frequency responses of the digital and continuous system are obtained from equations (41) and (42) by substituting $w = j\gamma$ and are given by

$$F_2(j\gamma) = \left. \frac{G_{c2}(j\omega)F_1(j\omega)G_2(j\omega)}{1+G_{c3}(j\omega)G_{c2}(j\omega)F_1(j\omega)G_2(j\omega)} \right|_{\omega=\frac{2}{T}\tan^{-1}\frac{\gamma T}{2}}$$

$$= A_2 + jB_2 \tag{46}$$

$$G_{d2}(j\gamma) = \frac{\frac{P_2+j\gamma Q_2}{1+L_2+j\gamma M_2}\left(X_{12}+jY_{12}\right)}{1+\frac{P_2+j\gamma Q_2}{1+L_2+j\gamma M_2}\left(X_{22}+jY_{22}\right)} \tag{47}$$

where

$$P_2 = a_{2,0}-a_{2,2}\gamma^2+a_{2,4}\gamma^4-a_{2,6}\gamma^6+ \cdots \tag{48}$$

$$Q_2 = a_{2,1}-a_{2,3}\gamma^2+a_{2,5}\gamma^4-a_{2,7}\gamma^6+ \cdots \tag{49}$$

$$L_2 = 0-b_{2,2}\gamma^2+b_{2,4}\gamma^4-b_{2,6}\gamma^6+ \cdots \tag{50}$$

$$M_2 = b_{2,1}-b_{2,3}\gamma^2+b_{2,5}\gamma^4-b_{2,7}\gamma^6+ \cdots \tag{51}$$

$$X_{12}+jY_{12} = \frac{j\gamma}{1+j\gamma\frac{T}{2}} \frac{1}{1+\overline{G_{h0}G_1}(z)D_1(z)} \left|_{z=\frac{1+\frac{wT}{2}}{1-\frac{wT}{2}}} \frac{G_1G_2(j\omega)}{j\omega}\right|_{\omega=\frac{2}{T}\tan^{-1}\frac{\gamma T}{2}} \tag{52}$$

$$X_{22}+jY_{22} = \frac{\overline{G_{h0}G_1G_2G_{c3}}(z)}{1+\overline{G_{h0}G_1}(z)D_1(z)} \left|_{z=\frac{1+j\gamma\frac{T}{2}}{1-j\gamma\frac{T}{2}}}\right. \tag{53}$$

The error function between $G_{d2}(j\gamma)$ and $F_2(j\gamma)$ which is to be minimized is given by

$$E_{m2} = \int_{\gamma_1}^{\gamma_2} \left[(A_2\sigma-B_2\tau-\phi)^2 + (A_2\tau+B_2\sigma-\theta)^2\right] d\gamma \tag{54}$$

where

$$\phi = P_2X_{12}+\gamma Q_2Y_{12} \tag{55}$$

$$\theta = P_2Y_{12}+\gamma Q_2X_{12} \tag{56}$$

$$\sigma = 1+L_2+P_2X_{22} \tag{57}$$

$$\tau = \gamma M_2+P_2Y_{22}+QX_{22} \tag{58}$$

Differentiating E_{m2} with respect to $a_{2,i}$'s and $b_{2,i}$'s and equating the resulting equations to zero represents (m+n+1) linear equations in (m+n+1) unknowns $a_{2,0}$ to $a_{2,m}$ and $b_{2,1}$ to $b_{2,n}$. Then equations can be written in the matrix form as given in equation (59)

$$\begin{bmatrix} a_{2,o} \\ a_{2,1} \\ a_{2,2} \\ a_{2,3} \\ \vdots \\ b_{2,1} \\ b_{2,2} \\ b_{2,3} \\ b_{2,4} \\ \vdots \end{bmatrix} = \begin{bmatrix} T_o & 0 & -T_2 & 0 & T_4 & 0 \cdots & V_1 & -U_2 & -V_3 & U_4 & V_5 & -U_6 & \cdots \\ 0 & T_2 & 0 & -T_4 & 0 & T_6 \cdots & U_2 & V_3 & -U_4 & -V_5 & U_6 & -V_7 & \cdots \\ -T_2 & 0 & T_4 & 0 & -T_6 & 0 \cdots & -V_3 & U_4 & V_5 & -U_6 & -V_7 & U_8 & \cdots \\ 0 & -T_4 & 0 & T_6 & 0 & -T_8 \cdots & -U_4 & -V_5 & U_6 & V_7 & -U_8 & -V_8 & \cdots \\ \vdots & & & & & & & & & & & & \\ V_1 & U_2 & -V_3 & -U_4 & V_5 & U_6 \cdots & W_2 & 0 & -W_4 & 0 & W_6 & 0 & \cdots \\ -U_2 & V_3 & U_4 & -V_5 & -U_6 & V_7 \cdots & 0 & W_4 & 0 & -W_6 & 0 & W_8 & \cdots \\ -V_3 & -U_4 & V_5 & U_6 & -V_7 & -U_8 \cdots & -W_4 & 0 & W_6 & 0 & -W_8 & 0 & \cdots \\ U_4 & -V_5 & -U_6 & V_7 & U_8 & -V_9 \cdots & 0 & W_6 & 0 & W_8 & 0 & -W_{10} & \cdots \\ \vdots & & & & & & & & & & & & \end{bmatrix}^{-1} \begin{bmatrix} -U_o \\ V_1 \\ U_2 \\ -V_3 \\ \vdots \\ 0 \\ W_2 \\ 0 \\ W_4 \\ \vdots \end{bmatrix} \tag{59}$$

where

$$T_h = \int_{\gamma_1}^{\gamma_2} \left[\left(A_2^2+B_2^2\right)\left(X_{22}^2+Y_{22}^2\right) + \left(X_{12}^2+Y_{12}^2\right) + 2B_2\left(X_{12}Y_{22}-X_{22}Y_{12}\right) - 2A_2\left(X_{12}X_{22}Y_{12}Y_{22}\right) \right] \gamma^h d\gamma \tag{60}$$

$$U_h = \int_{\gamma}^{\gamma_2} \left(A_2^2+B_2^2\right)X_{22} - \left(A_2X_{12}+BY_{12}\right)\gamma^h d\gamma \tag{61}$$

$$V_h = \int_{\gamma_1}^{\gamma_2} \left(A_2^2+B_2^2\right)Y_{22} + \left(B_2X_{12}-A2_{12}\right)\gamma^h d\gamma \tag{62}$$

$$W_h = \int_{\gamma_1}^{\gamma_2} \left(A_2^2+B_2^2\right)\gamma^h d\gamma \tag{63}$$

Equations (59)-(63) provide a design algorithm which has been programmed on a digital computer, IBM (370/3031) and is available in the form of a subroutine written in FORTRAN IV. The pulse transfer function of the digital controller, $D_2(z)$, can now be obtained as

$$D_2(z) = D_2(w)\Big|_{w=\frac{2}{T}\frac{z-1}{z+1}} \tag{64}$$

3. Digital Controller, $D_3(z)$, in the Feedback Path of Outer Loop

The block diagram of the digital control system after replacing the continuous compensators $G_{c1}(s)$ and $G_{c2}(s)$ with already designed digital controllers and after replacing $G_{c3}(s)$ with yet to be designed digital controller $D_3(z)$ is shown in Figure 5.

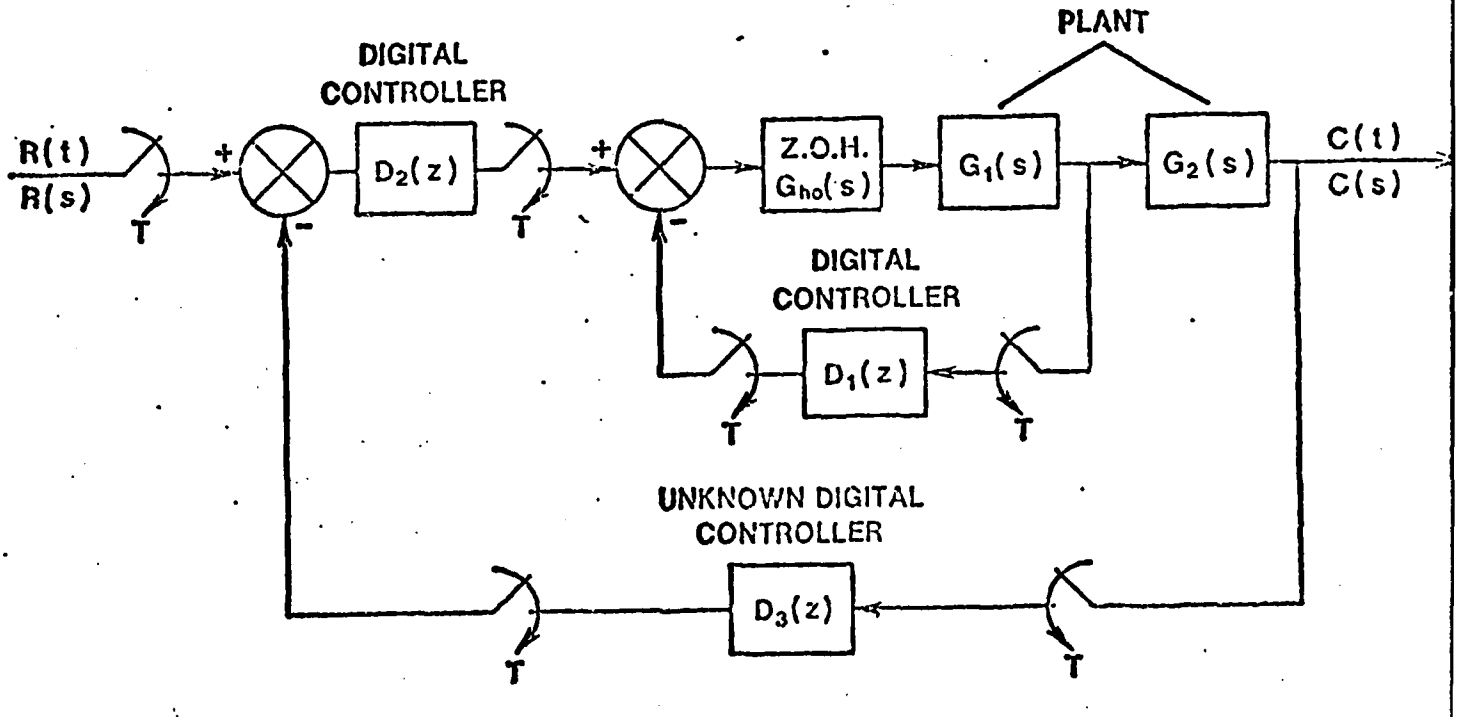

Figure 5. Digital Control System with unknown digital controller in the feedback loop.

The overall transfer function of the digital control system shown in Figure 5 can be written in the w-domain as

$$G_{d3}(w) = \frac{w}{1+\frac{wT}{2}} \frac{\dfrac{D_2(z)}{1+\overline{G_{h0}G_1}(z)D_1(z)}}{1+D_3(z)\dfrac{D_2(z)\overline{G_{h0}G_1G_2}(z)}{1+\overline{G_{h0}G_1}(z)D_1(z)}} \Bigg|_{z=\frac{1+\frac{wT}{2}}{1-\frac{wT}{2}}} \frac{G_1G_2(s)}{s} \Bigg|_{s=j\frac{2}{T}\tan^{-1}\frac{wT}{2j}} \tag{65}$$

Let the transfer function of the digital controller $D_3(w)$ be written in the w-domain as

$$D_3(w) = \frac{a_{3,m}w^m + a_{3,m-1}w^{m-1} + \cdots + a_{3,1}w + a_{3,0}}{b_{3,n}w^n + b_{3,n-1}w^{n-1} + \cdots + b_{3,1}w + b_{3,0}}, \quad m \leq n \tag{66}$$

where $a_{3,i}$'s and $b_{3,i}$'s are constants to be determined. Since the digital controller $D_3(z)$ is located in the feedback path, these constants can be determined using the design algorithm developed for $D_1(z)$, equations (36)-(41), where

$$A_1 = A_2 \tag{67}$$

$$B_1 = B_2 \tag{68}$$

$$X_{11}+jY_{11} = \frac{w}{1+\frac{wT}{2}} \frac{D_2(z)}{1+\overline{G_{h0}G_1}(z)D_1(z)} \Bigg|_{z=\frac{1+\frac{wT}{2}}{1-\frac{wT}{2}}} \frac{G_1G_2(s)}{s} \Bigg|_{s=j\frac{2}{T}\tan^{-1}\frac{\gamma T}{2}} \tag{69}$$

$$X_{21}+jY_{21} = \frac{D_2(z)\overline{G_{h0}G_1G_2}(z)}{1+\overline{G_{h0}G_1}(z)D_1(z)} \Bigg|_{z=\frac{1+\frac{wT}{2}}{1-\frac{wT}{2}}} \tag{70}$$

Finally, we would like to point out here that using the design algorithm developed for the digital controllers in the feedforward and feedback path, we can convert any existing multiloop continuous control system into a multiloop digital control system.

SECTION IV

NUMERICAL EXAMPLES

1. Numerical Example 1

The first example considered in this report is to convert an existing single loop continuous control system shown in Figure 6 into a digital control system shown in Figure 7.

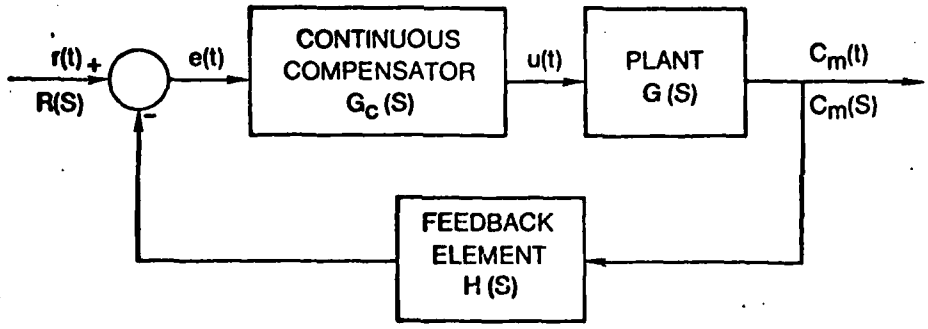

Figure 6. Existing single-loop continuous-data control system for Example 1.

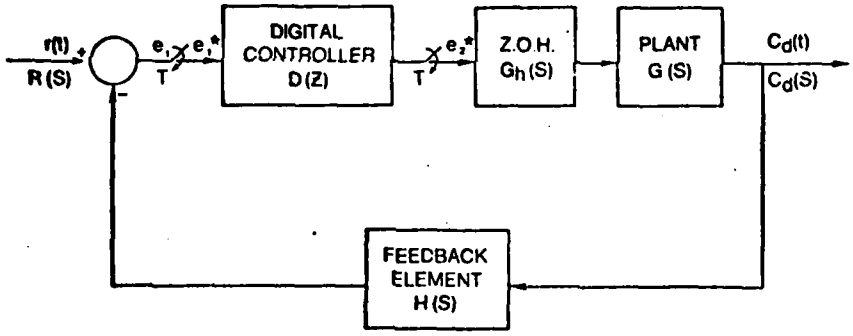

Figure 7. Redesigned digital control system for Example 1.

The transfer function of the continuous controller, plant and the feedback element is given by

$$G_c(s) = \frac{1+0.416s}{1+0.139s} \tag{71}$$

$$G(s) = \frac{10}{s(s+1)} \tag{72}$$

$$H(s) = 1 \tag{73}$$

Using equations (71)-(73), the overall transfer function of the continuous model can be written as

$$F(s) = \frac{G_c(s)G(s)}{1+G_c(s)G(s)H(s)} = \frac{29.93s + 71.942}{s^3+8.194s^2+37.12s+71.942} \tag{74}$$

The magnitude of the frequency response of the continuous model is obtained using equation (74) and is shown in Figure 8.

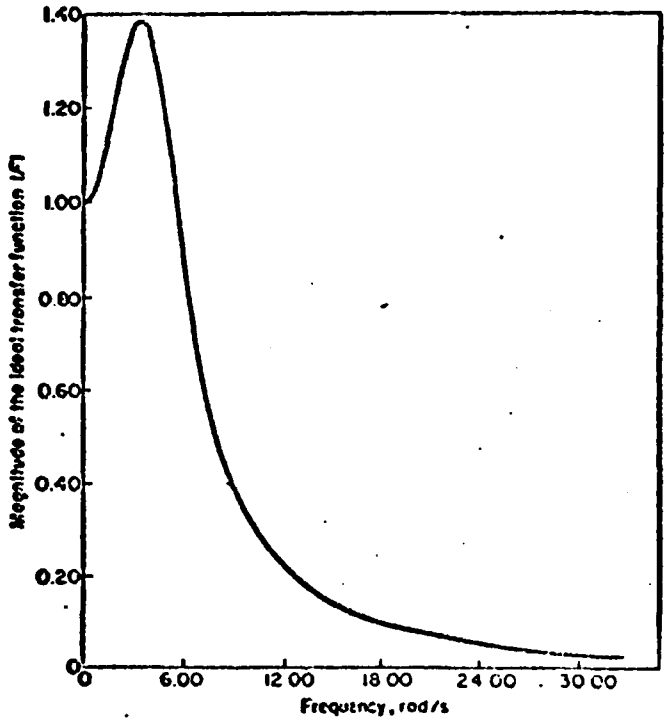

Figure 8. Magnitude of the frequency response of the continuous system of example 1.

Based on the frequency response, the sampling period T is selected to be 0.15s. From equations (72)-(73),

$$G_h GH(s) = \frac{10(1-e^{-sT})}{s^2(s+1)} \tag{75}$$

The z-transform associated with this transfer function is given by

$$G_h GH(z) = \frac{0.10708z+0.101858}{z^2-1.8607z+0.8607} \tag{76}$$

Substituting $z = \frac{1+j\gamma\frac{T}{2}}{1-j\gamma\frac{T}{2}}$ in equation (76) we get

$$G_h GH(j\gamma) = X_{22}+jY_2 = \left.\frac{9.981-.73w-.0019w^2}{w(w+.998)}\right|_{w=j\gamma} \tag{77}$$

From Figure 7 and equation (72), we get

$$X_{12}+jY_{12} = \left.\frac{j\gamma}{1+j\gamma\frac{T}{2}}\frac{G(s)}{s}\right|_{s=j\frac{2}{T}\tan^{-1}\frac{\gamma T}{2}} = \left.\frac{j\gamma}{1+j\gamma\frac{T}{2}}\frac{10}{s^2(s+1)}\right|_{s=j\frac{2}{T}\tan^{-1}\frac{\gamma T}{2}} \tag{78}$$

Also

$$A_2+jB_2 = \left.\frac{29.93s+71.942}{s^3+8.194s+37.12s+71.942}\right|_{s=j\frac{2}{T}\tan^{-1}\frac{\gamma T}{2}} \tag{79}$$

Equations (77)-(79) are the only information required to design a digital controller for the digital control system shown in Figure 7. Feeding these equations to the computer program written for equations (59)-(63), the transfer function of the first-order digital controller given by the algorithm in the w-domain is

$$D(w) = \frac{.59713 + .3636w}{1+.13053w} \tag{80}$$

Substituting $w = \frac{2}{T}\frac{z-1}{z+1}$ in equation (80) gives the pulse-transfer function of the digital controller

$$D(z) = \frac{1.9865 - 1.55074}{z-.27108} \tag{81}$$

The frequency responses of the existing continuous system and the digital control system with the digital controller given by equation (81) are shown in Figures 9-11. It can be seen that both the magnitude and phase angle of

the digital system matches closely with that of the continuous model. If the designer is not satisfied with the results and wants to improve the performance, the only change which need to be made is to increase the order of the digital controller. The algorithm goes through the standard steps given above and finds the parameters of the new digital controller. Thus the performance may be improved at the expense of increasing complexity.

2. Comparison with the existing methods

The digital controller for the digital control system discussed in the numerical example is redesigned using the Tustin transform[12] (bilinear transformation); methods presented by Tabak[1] (prewarped bilinear transformation) and by the author of the paper and Yeh[5] (discrete frequency matching). Using these methods, the continuous controller given in equation (71) is converted into digital controllers and are given by

Tustin transform:

$$D(z) = \frac{2.294z-1.5936}{z-.299} \tag{82}$$

Prewarped bilinear transform:

$$D(z) = \frac{2.42965z-1.68046}{z-0.2509} \tag{83}$$

Using the method presented by the author and Yeh:

first-order:

$$D(z) = \frac{3.6787z-2.31256}{z+0.383656} \tag{84}$$

second order:

$$D(z) = \frac{3.96z^2-3.65z+0.56}{z^2-0.34z-0.384} \tag{85}$$

The frequency responses of the digital control system with digital controllers given by equations (82)-(85) are shown in Figures 9-11. Comparison of the results in these figures demonstrate that the digital controller obtained by the present method gives better results. The unit step responses of the continuous model and digital control systems obtained by different methods are shown in Figure 12. It can be seen from this figure that the present method gives better results.

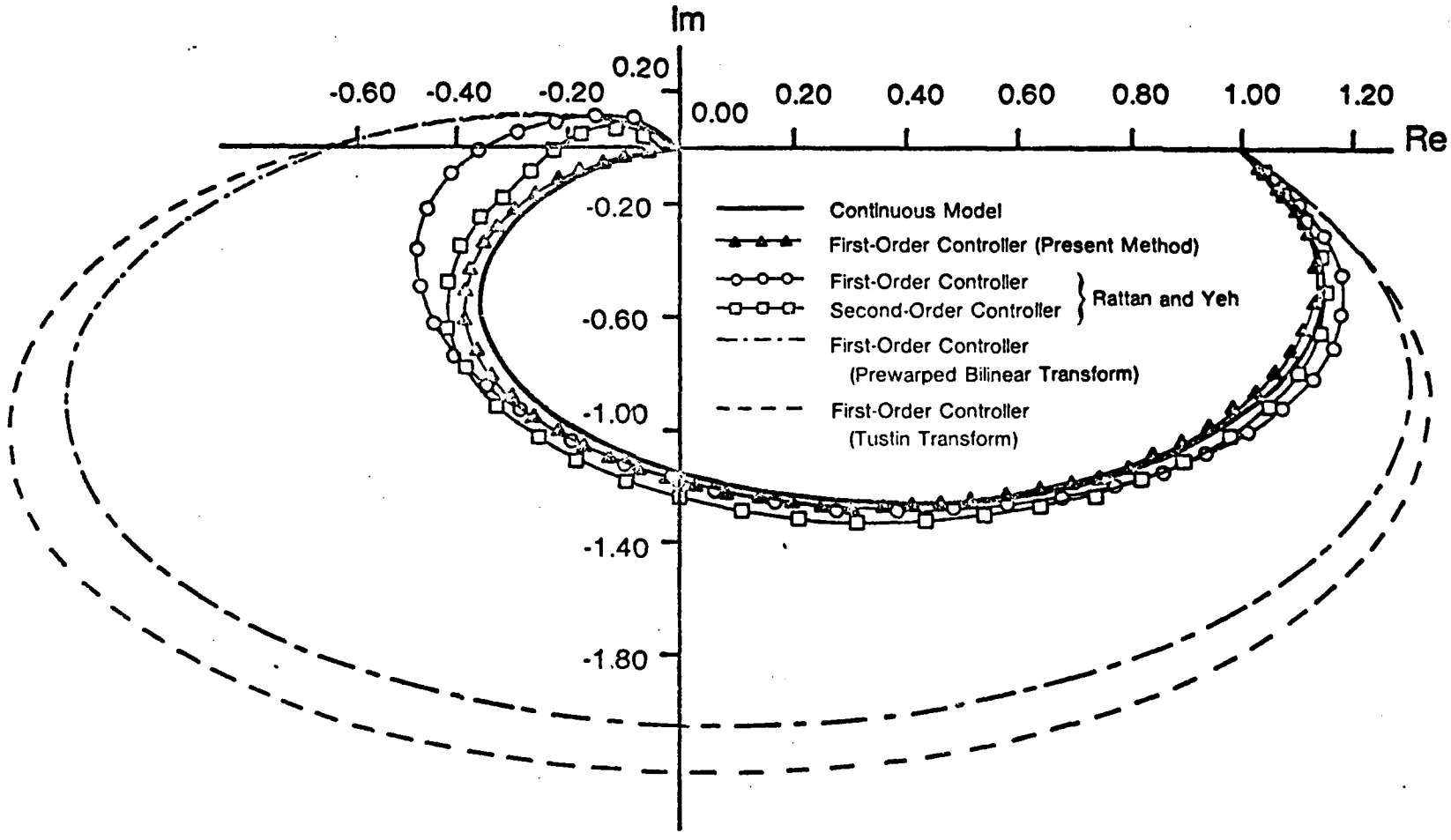

Figure 9. Nyquist plot of the frequency responses of the continuous model and the digital control system designed by different methods (example 1).

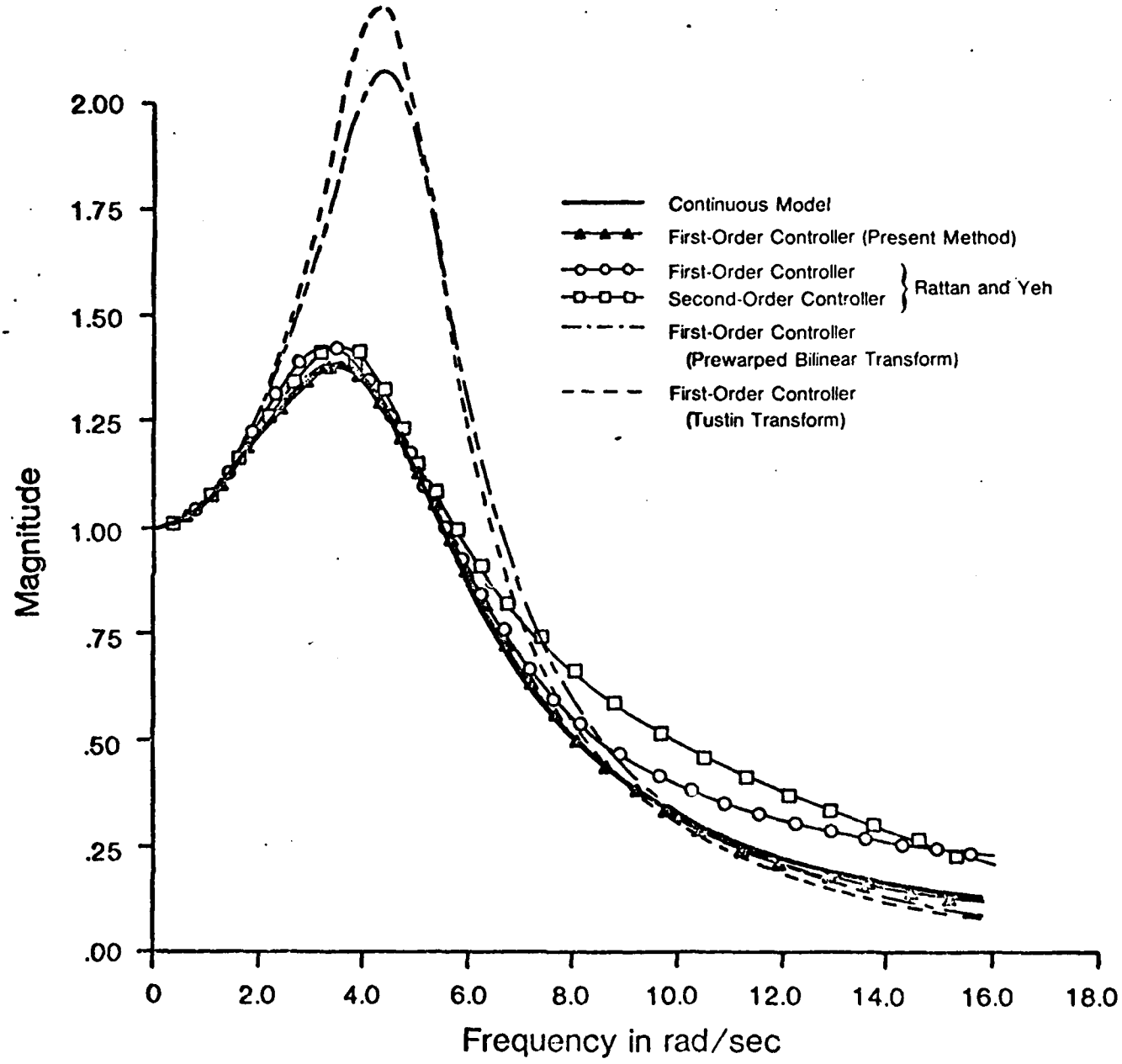

Figure 10. Magnitude plot of the frequency responses of the continuous model and the digital control system designed by different methods. (example 1).

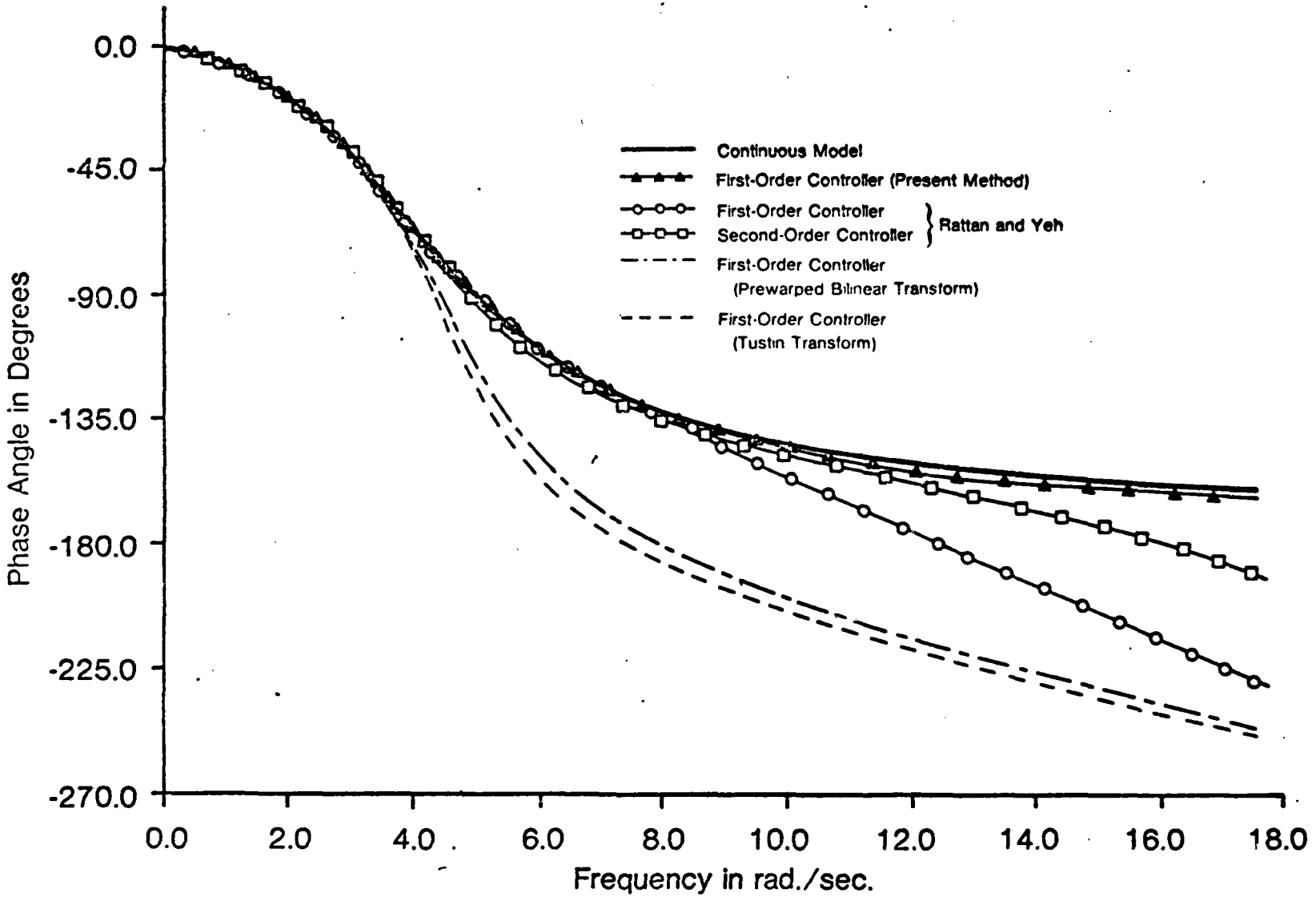

Figure 11. Phase plot of the frequency responses of the continuous model and the digital control system designed by different methods (example 1).

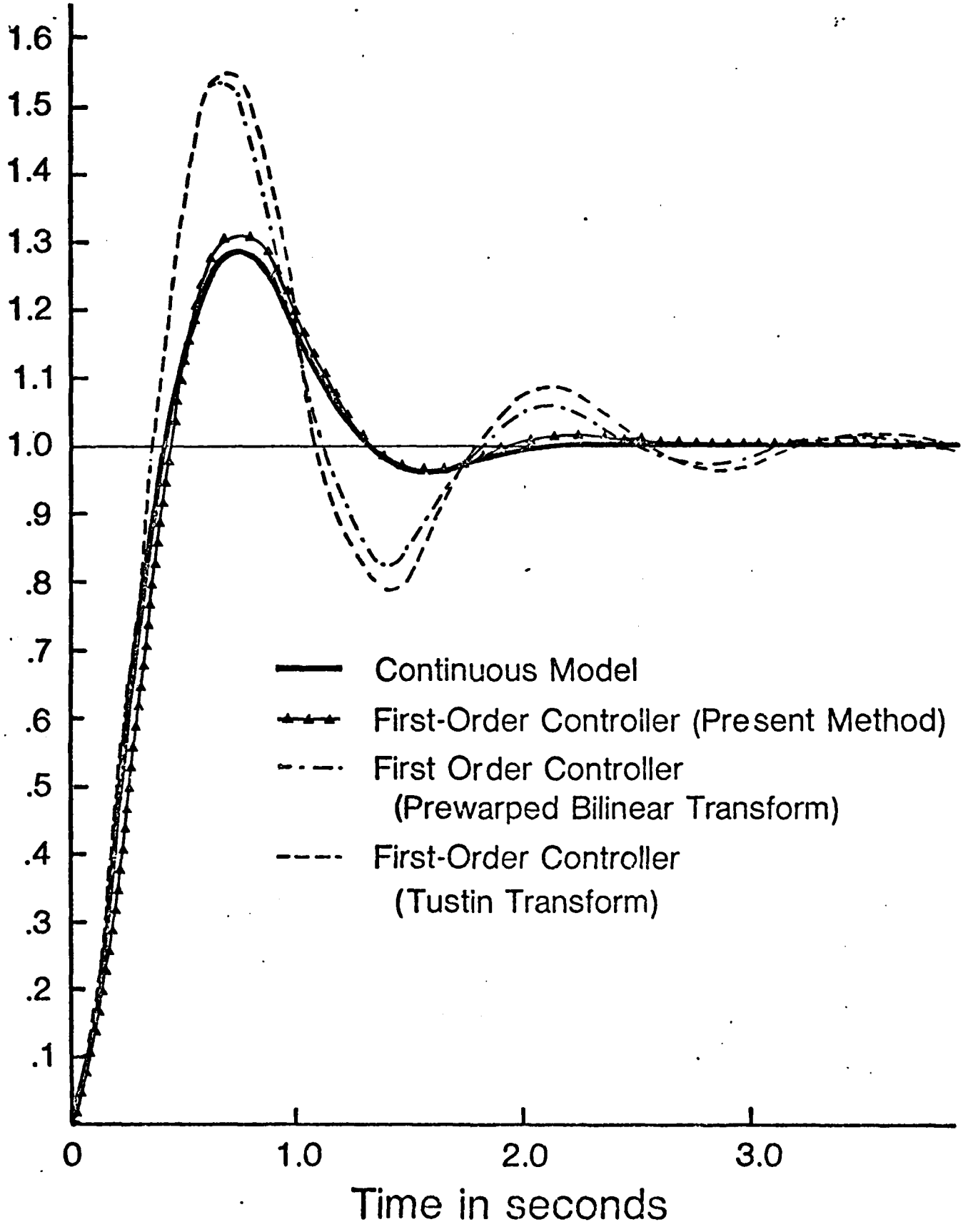

Figure 12. Unit step responses of the continuous model and the digital control system designed by different methods (example 1).

3. Numerical Example 2

The digitalization techniques, described in section III was applied to an analog flight controller[13] for the longitudinal YF-16 as shown in Figure 13. A listing of transfer functions of the aircraft flight at 30,000 ft at M = 0.6 can be found in Appendix A.

The problem is to digitalize, i.e., to replace the continuous-time controllers by digital controllers while preserving the dynamic properties of the whole system. The block diagram of the digitally controlled YF-16 obtained by inserting a sampler at the input of the actuator and replacing continuous controllers by digital controllers is shown in Figure 14.

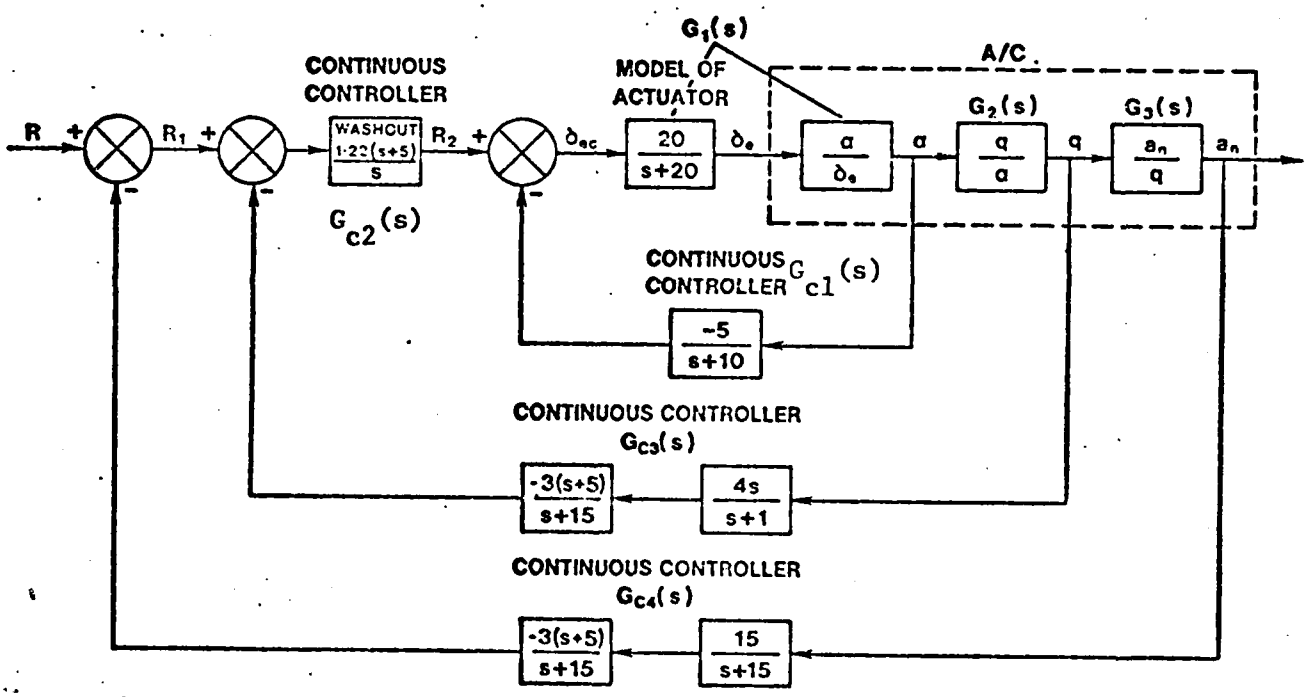

Figure 13. Analog YF-16 controller (M=0.6, h=30,000 ft)

$D_1(z)$ Controller: From Figure 13, the transfer function of the continuous model (innermost loop) for the design of digital controller $D_1(z)$ can be written as

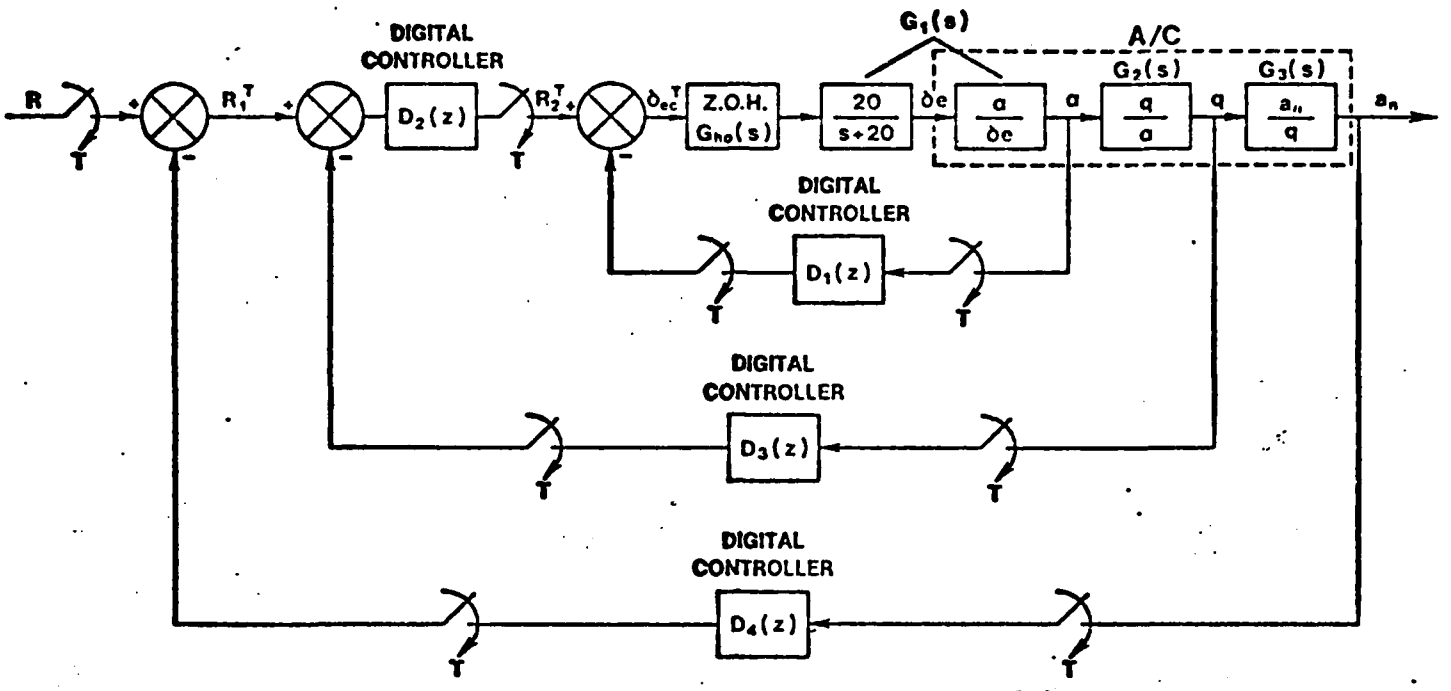

Figure 14. Digital YF-16 controller.

$$F_1(s) = \frac{\alpha(s)}{R_2(s)} = \frac{G_1(s)}{1+G_{c1}(s)G_1(s)}$$

$$= -\frac{1.45S^4+162.1S^3+1478.S^2+24.53S+8.3}{S^6+30.95S^5+226.2S^4+127.7S^3+270.5S^2+3.75S+1.31} \tag{86}$$

In view of the innermost loop of Figure 14 and equation (19), we have

$$X_{11}+jY_{11} = \frac{j\gamma}{1+j\gamma\frac{T}{2}} \frac{20}{S+20} \frac{\alpha}{\delta_e}(s)\Bigg|_{s = j\frac{2}{T}\tan^{-1}\frac{\gamma T}{2}} \tag{87}$$

$$G_{h0}G_1(s) = \frac{1-e^{-st}}{S} \frac{20}{s+20} \frac{\alpha}{\delta_e}(s) \tag{88}$$

The z-transform associated with this transfer function is given by

$$G_{h0}G_1(z) = \frac{.0022z^4-.00034z^3-.0057z^2+.0037z+.000175}{z^5-4.41z^4+7.68z^3-6.54z^2+2.71z-.4326} \tag{89}$$

Substituting $Z = \frac{1+\gamma\frac{T}{2}}{1-\gamma\frac{T}{2}}$ in equation (89), we get

$$G_h G_1(j\gamma) = x_{21}+jY_{21} = \frac{.0029w^5-.05w^4-1.04w^3+140.1w^2+2.24w-.79}{w^5+19.9w^4+15.7w^3-44.3w^2-.74w-.27}\Bigg|_{w=j\gamma} \quad (90)$$

Feeding equations (86), (87) and (90) to the computer program written for the algorithm implementing equations (36)-(40), the transfer function of the first-order digital controller D_1 in the w-domain is given by

$$D_1(w) = \frac{0.501+.0109w}{1+.1007w} \quad (91)$$

substituting $w = \frac{2}{T}\frac{z-1}{z+1}$ in equation (91), we get

$$D_1(z) = \frac{.1732z-.0072}{z-.668} \quad (92)$$

The frequency response of the innermost loop of the digital control system shown in Figure 14 with the digital controller given by Equation (92) is shown in Figures 15, 16, 17. To compare the result, digital controllers are also obtained by the other methods and their pulse-transfer function are given by

Tustin transform:

$$D_1(z) = \frac{.083(z+1)}{z-.667} \quad (93)$$

Discrete frequency matching method:

$$D_1(z) = \frac{.3659(z-.7974)}{z-.8553} \quad (94)$$

The frequency responses obtained using the digital controllers given by equations (93) and (94) are also plotted on Figures 15, 16, 17. Comparison of these results demonstrate that the digital controller obtained by the present method gives better results.

$D_2(z)$ Controller: From Figure 13, the transfer function of the continuous model for the design of digital controller $D_2(z)$ can be written as

$$F_2(s) = \frac{q(s)}{R_1(s)} = \frac{G_{c2}(s)F_1(s)G_2(s)}{1+G_{c3}(s)G_{c2}(s)F_1(s)G_2(s)}$$

$$= -\frac{180s^6+.568\times10^4s^5+.579\times10^5s^4+.214\times10^6s^3+.234\times10^6s^2+.73\times10^5s+629.9}{s^8+447s^7+1925s^6+.86\times10^4s^5+.35\times10^5s^4+.75\times10^5s^3+.33\times10^5s^2+329\ 1s+19.6} \quad (95)$$

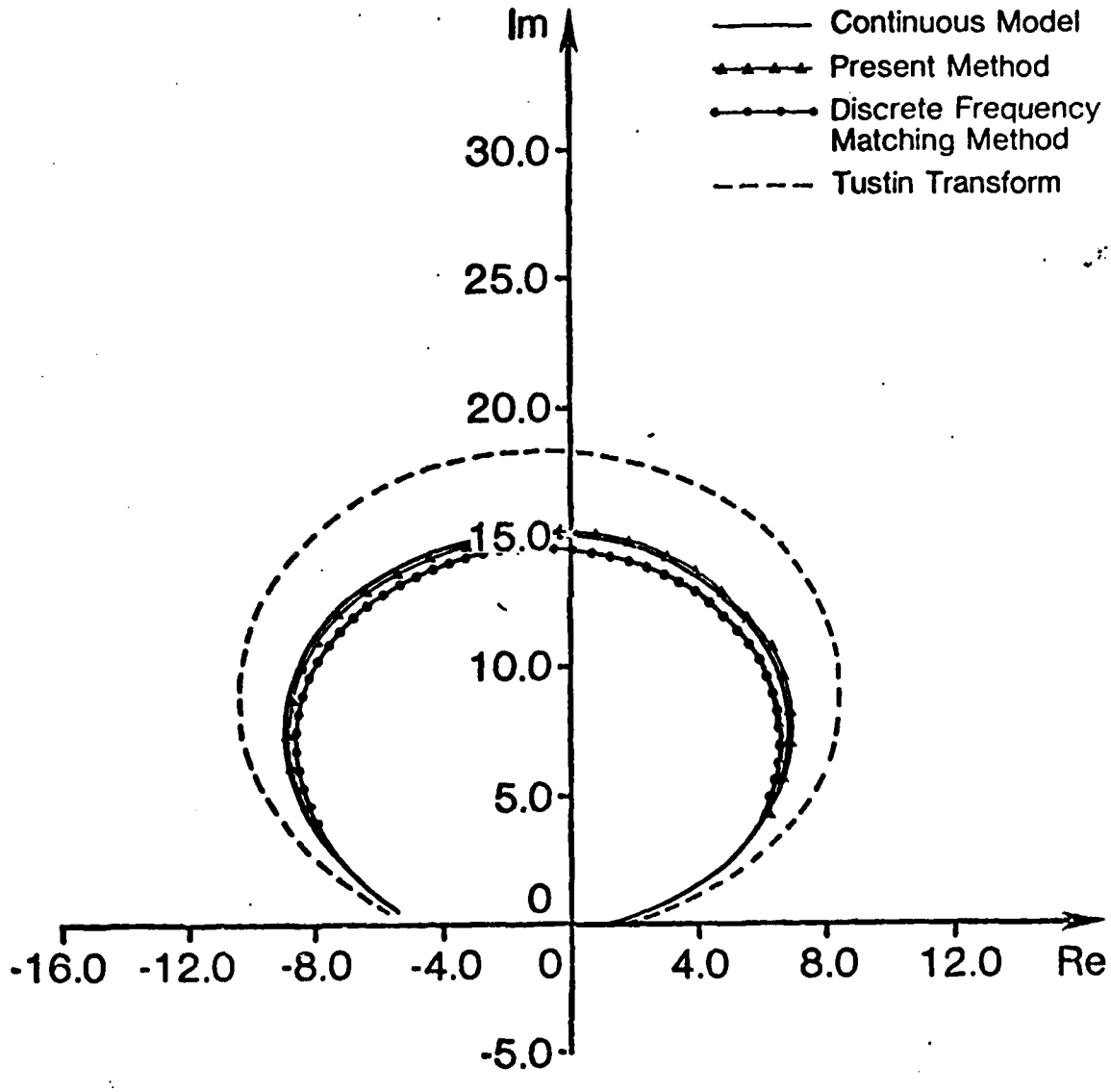

Figure 15. Nyquist plot of the frequency responses of the innermost loop of the continuous system and the corresponding digital control system designed by different methods, (example 2).

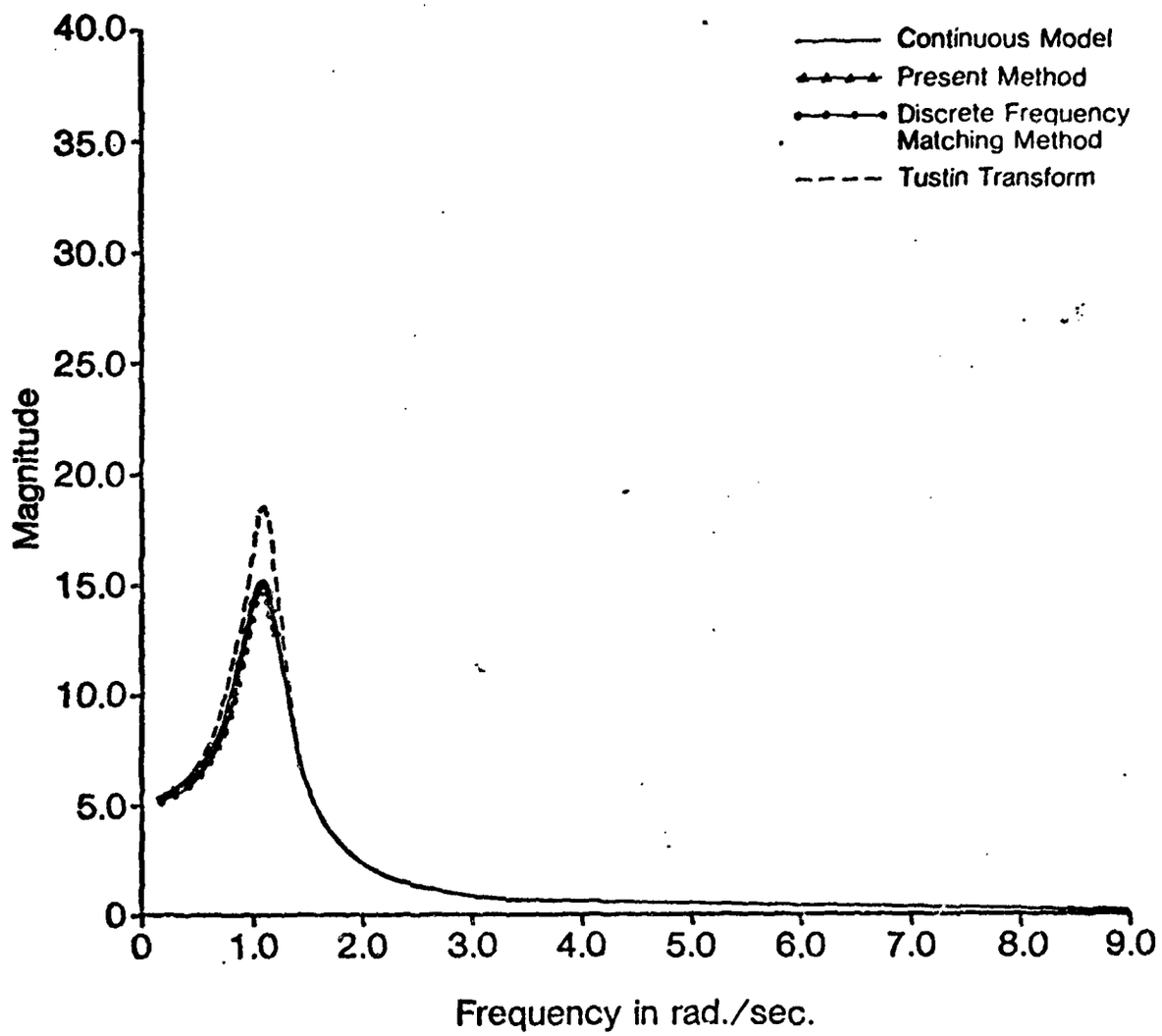

Figure 16. Magnitude plot of the frequency responses of the innermost loop of the continuous system and the corresponding digital control system designed by different methods (example 2).

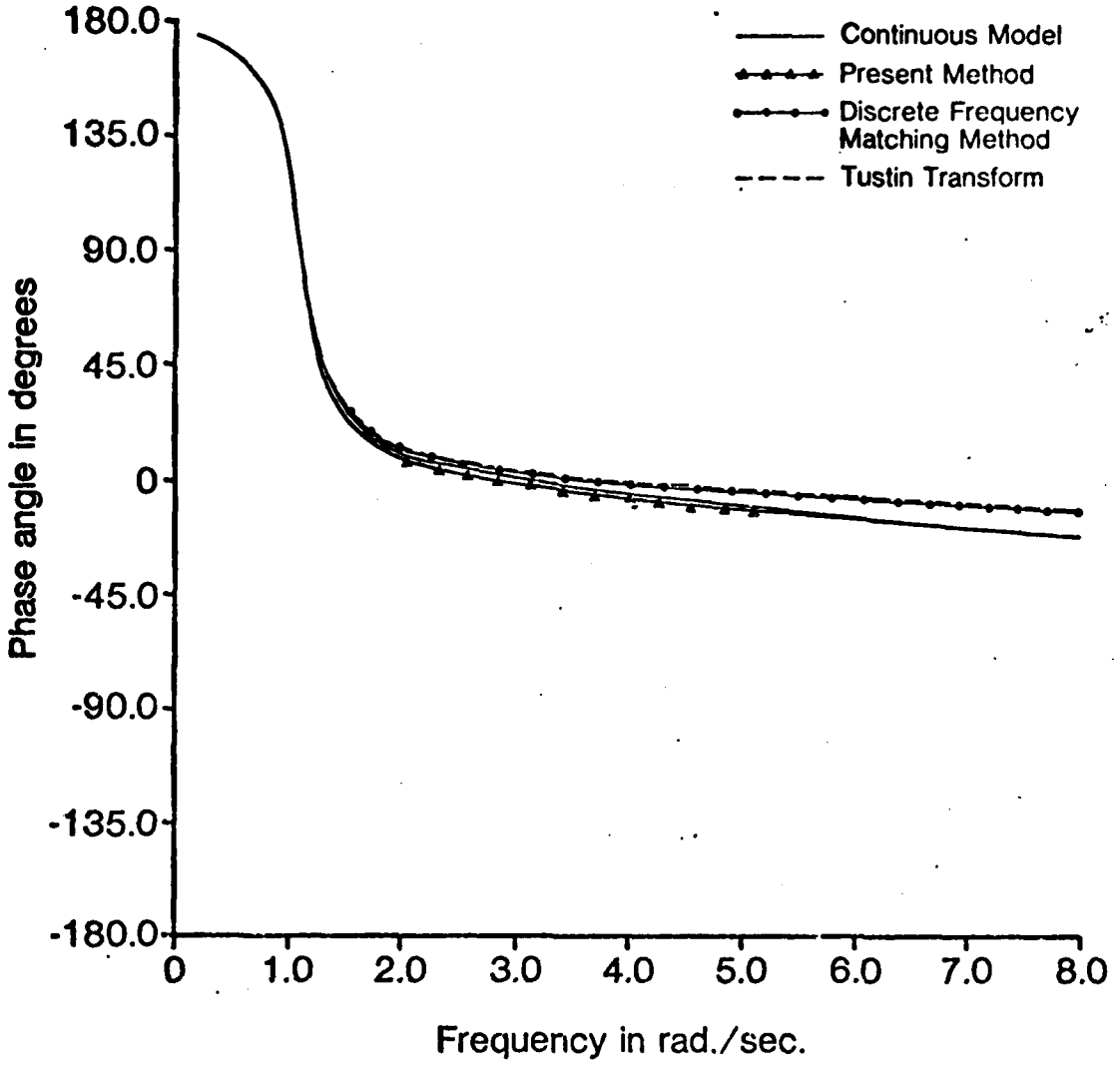

Figure 17. Phase plot of the frequency responses of the innermost loop of the continuous system and the corresponding digital control system designed by different methods (example 2).

In view of Figure 14 and equation (53), we can write

$$X_{12}+jY_{12} = \frac{j\gamma}{1+j\gamma\frac{T}{2}} \frac{1}{1+G_{h0}G_1(w)D_1(w)}\Bigg|_{z=\frac{1+j\gamma\frac{T}{2}}{1-j\gamma\frac{T}{2}}} \frac{20}{s+20}\frac{q}{\delta e}(s)\Bigg|_{s=j\frac{2}{T}\tan^{-1}\frac{\gamma T}{2}} \tag{96}$$

$$G_{ho}G_1G_2G_{c3}(s) = -\frac{1-e^{-ST}}{S}\frac{24S(S+5)}{(S+1)(S+15)(S+20)}\frac{q}{\delta e} \tag{97}$$

From the z-transform of this transfer function and equations (90) and (91), we get

$$X_{22}+jY_{22} = \frac{1}{1+\overline{G_{h0}G_1}(w)D_1(w)} \frac{.00003w^6-.004w^5-.36w^4+10.5w^3+690.7w^2+11.1w+3.9}{w^6+29.8w^5+212.1w^4+110.6w^3-436.7w^2-7.6w-2.6}\Bigg|_{w=j\gamma} \tag{98}$$

Feeding equations (95), (96) and (98) to the computer program implementing equations (60)-(64), the transfer function of the digital controller D_2 in the w-domain is given by.

$$D_2(w) = 1.29 + \frac{5.45}{w} \tag{99}$$

Substituting $w = \frac{2}{T}\frac{z-1}{z+1}$ in equation (99), we get

$$D_2(z) = \frac{1.399z-1.181}{(z-1)} \tag{100}$$

The pulse-transfer functions of $D_2(z)$ obtained by the existing methods are given by

Tustin transform:

$$D_2(z) = \frac{1.342(z-.8182)}{(z-1)} \tag{101}$$

Discrete frequency matching method:

$$D_2(z) = \frac{1.3837(z-.80235)}{(z-1)} \tag{102}$$

The frequency responses of the middle loop of the continuous system shown in Figure 13 and the digital control system shown in Figure 14 with digital controllers $D_2(z)$ given by equations (100)-(102) are shown in Figures 18, 19 and 20. Comparing these results reveals that the digital controller obtained by the present method gives better results.

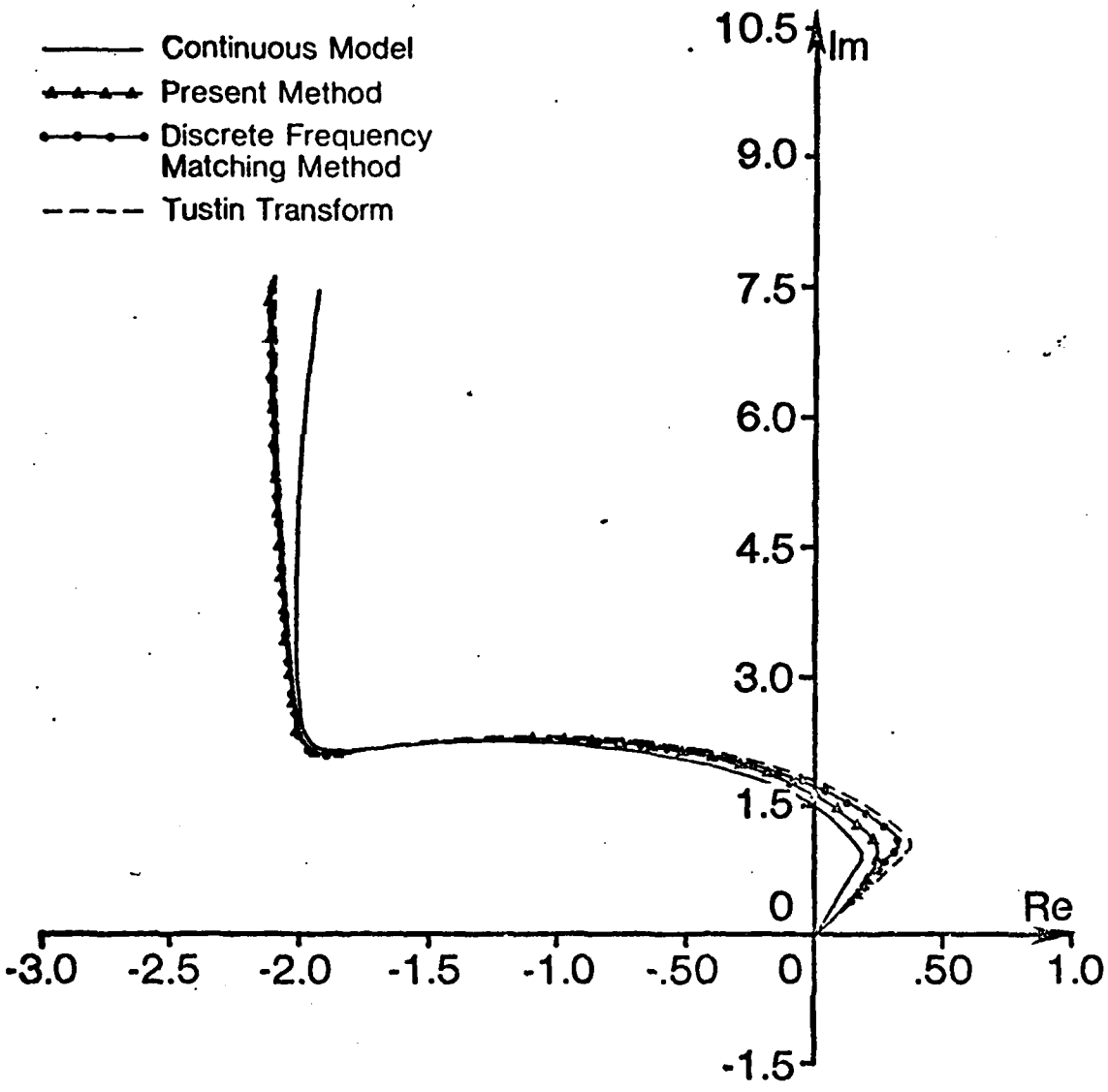

Figure 18. Nyquist plot of the frequency responses of the middle loop of the continuous system and the corresponding digital control system designed by different methods (example 2).

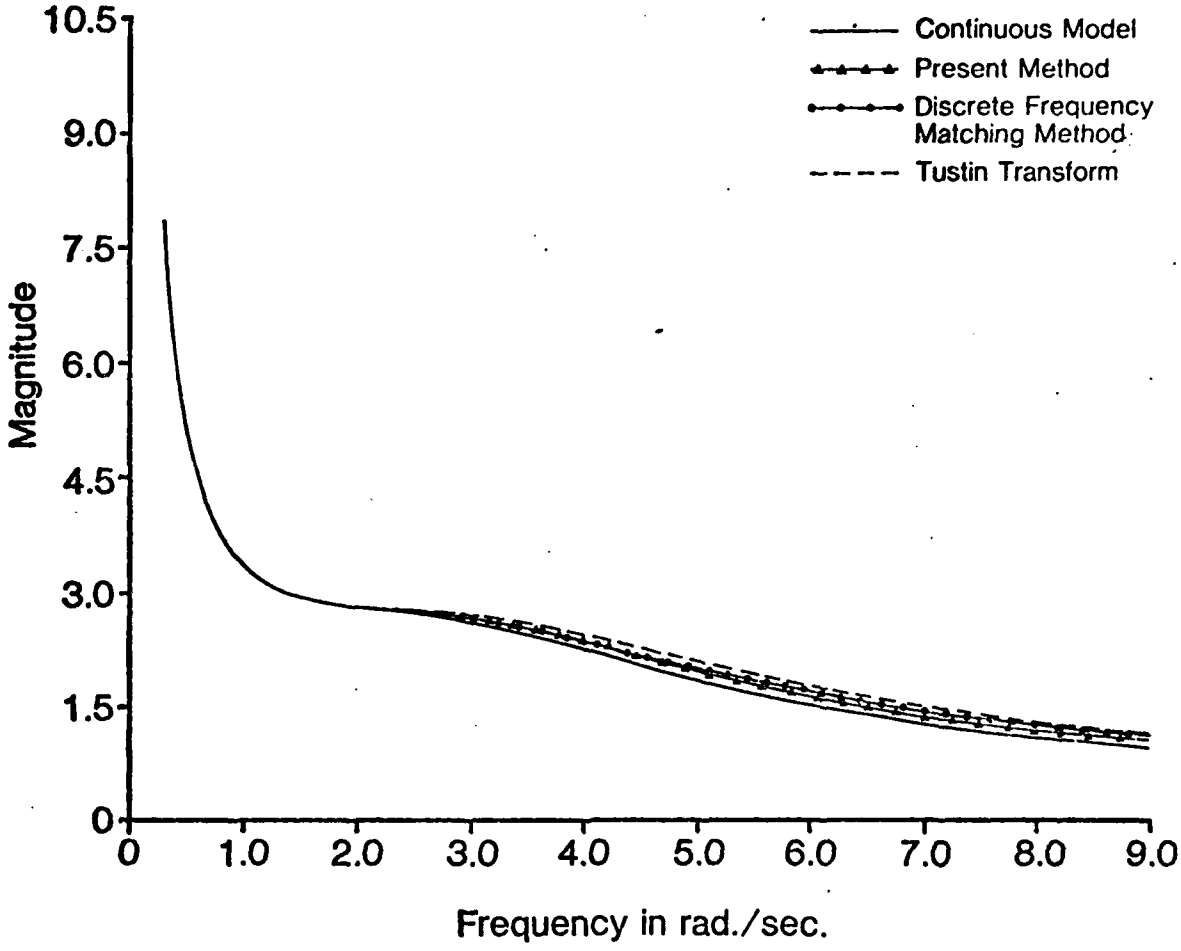

Figure 19. Magnitude plot of the frequency responses of the middle loop of the continuous system and the corresponding digital control system designed by different methods (example 2).

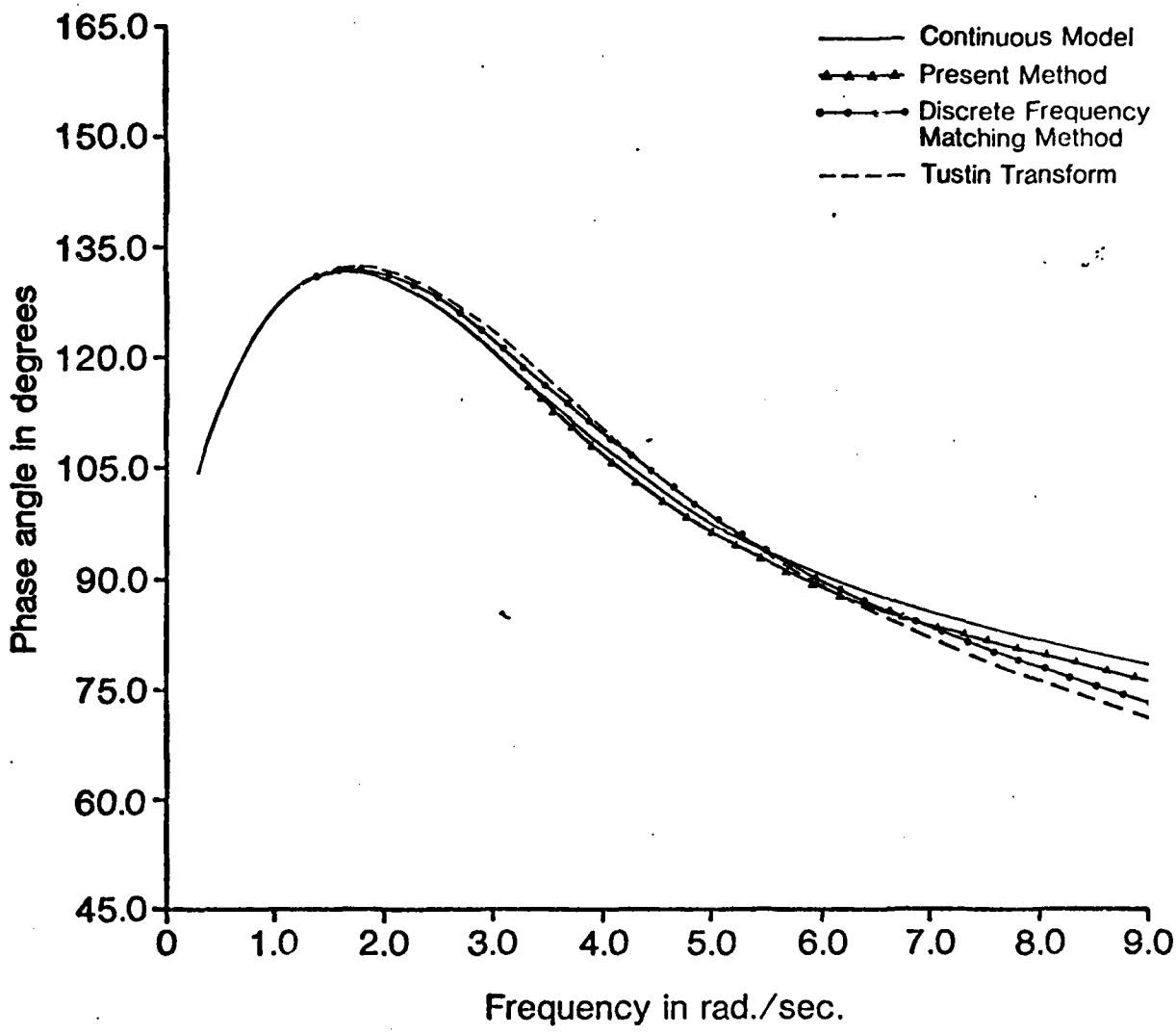

Figure 20. Phase plot of the frequency responses of the middle loop of the continuous system and the corresponding digital control system designed by different methods (example 2).

$D_3(z)$Controller

From Figure 14 and equations (70) and (71), we can write

$$X_{11}+jY_{11} = \frac{j\gamma}{1+j\gamma\frac{T}{2}} \frac{D_2(w)}{1+\overline{G_{h0}G_1}(w)D_1(w)}\bigg|_{w=j\gamma} \frac{20}{s+20}\frac{q}{\delta e}(s)\bigg|_{s=j\frac{2}{T}\tan^{-1}\gamma\frac{T}{2}} \tag{103}$$

and

$$X_{21}+jY_{21} = \frac{D_2(w)}{1+\overline{G_{h0}G_1}(w)D_1(w)} \frac{-.14w^4+7.3w^3+3.97w^2+.034w}{w^4+.95w^3-2.33w^2-.038w-.014}\bigg|_{w=j\gamma} \tag{104}$$

Feeding equations (95), and (103) and (104) to the computer program implementing equations (36)-(40), the transfer function of the digital controller $D_3(w)$ is given by

$$D_3(w) = \frac{w(0.41+096w)}{1+1.07w+.106w^2} \tag{105}$$

substituting $w = \frac{2}{T}\frac{z-1}{z+1}$ in equation (105), we get

$$D_3(z) = \frac{.8151z^2-1.502z+.687}{z^2-1.652z+.6646} \tag{106}$$

The pulse transfer functions of $D_3(z)$ obtained by the previous methods are given by

Tustin transform:

$$D_3(z) = \frac{0.995z^2-1.81z+.814}{z^2-1.5z+.517} \tag{107}$$

Discrete frequency matching method:

$$D_3(z) = \frac{1.5433(z-.8512)(z-1)}{(z-.3876)(z-.9652)} \tag{108}$$

The frequency responses of the middle loop of the continuous system shown in Figure 13 and the digital control system shown in Figure 14 with digital controller $D_3(z)$ given by equations (106)-(108) are shown in Figures 21, 22 and 23. Comparison of these results shows that the present method gives better results.

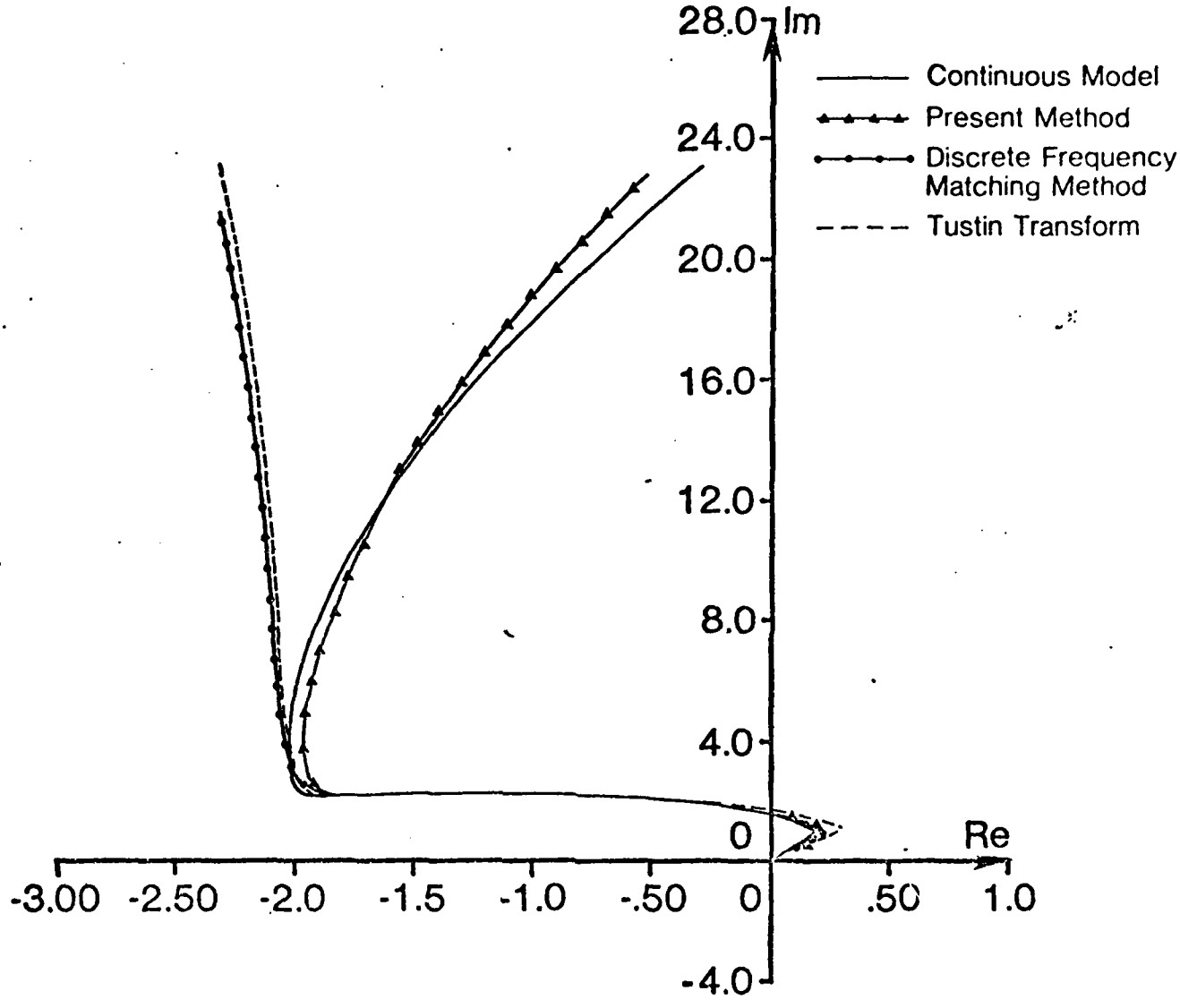

Figure 21. Nyquist plot of the frequency responses of the middle loop of the continuous system and the corresponding digital control system designed by different methods (example 2).

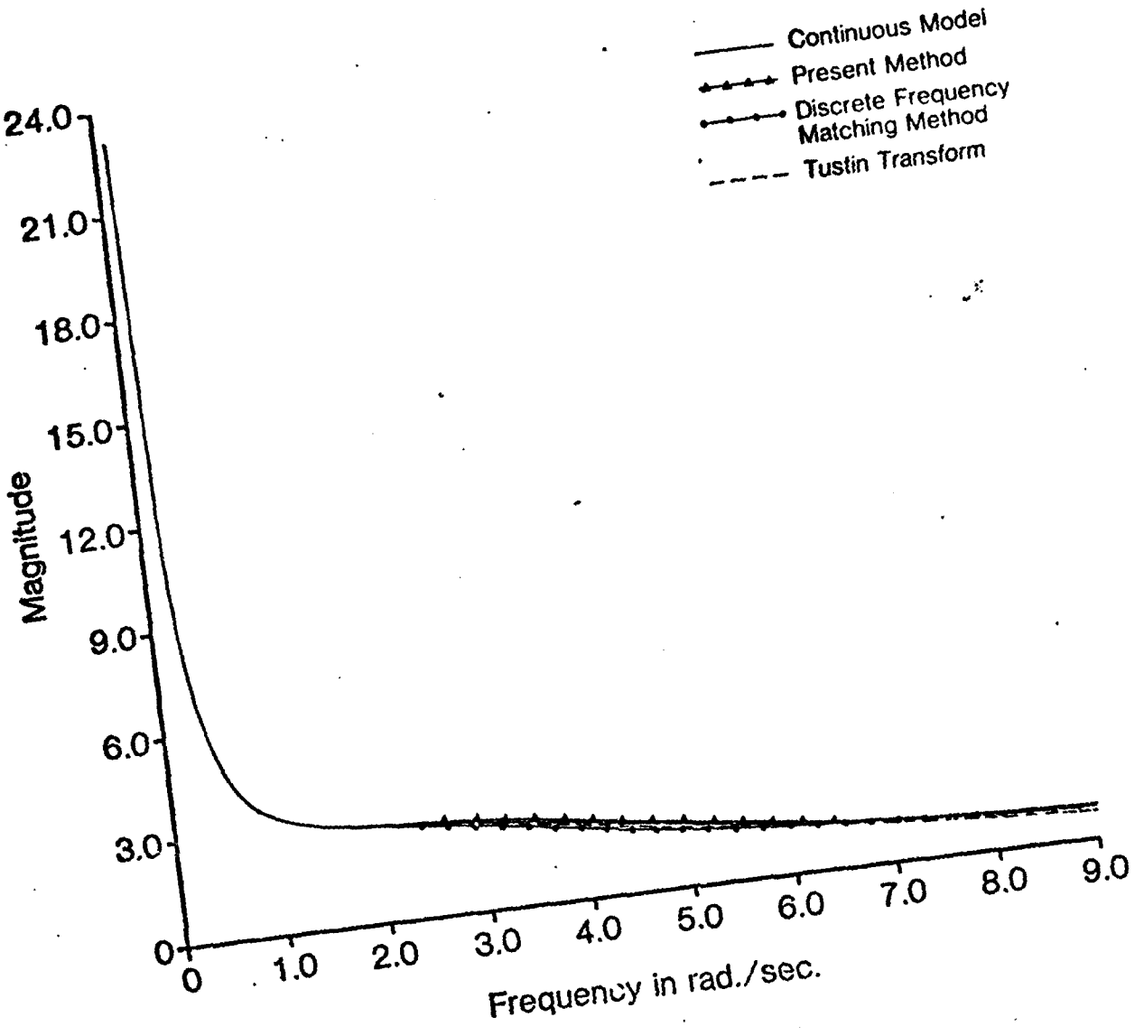

Figure 22. Magnitude Plot of the frequency responses of the middle loop of the continuous system and the corresponding digital control system designed by different methods (example 2).

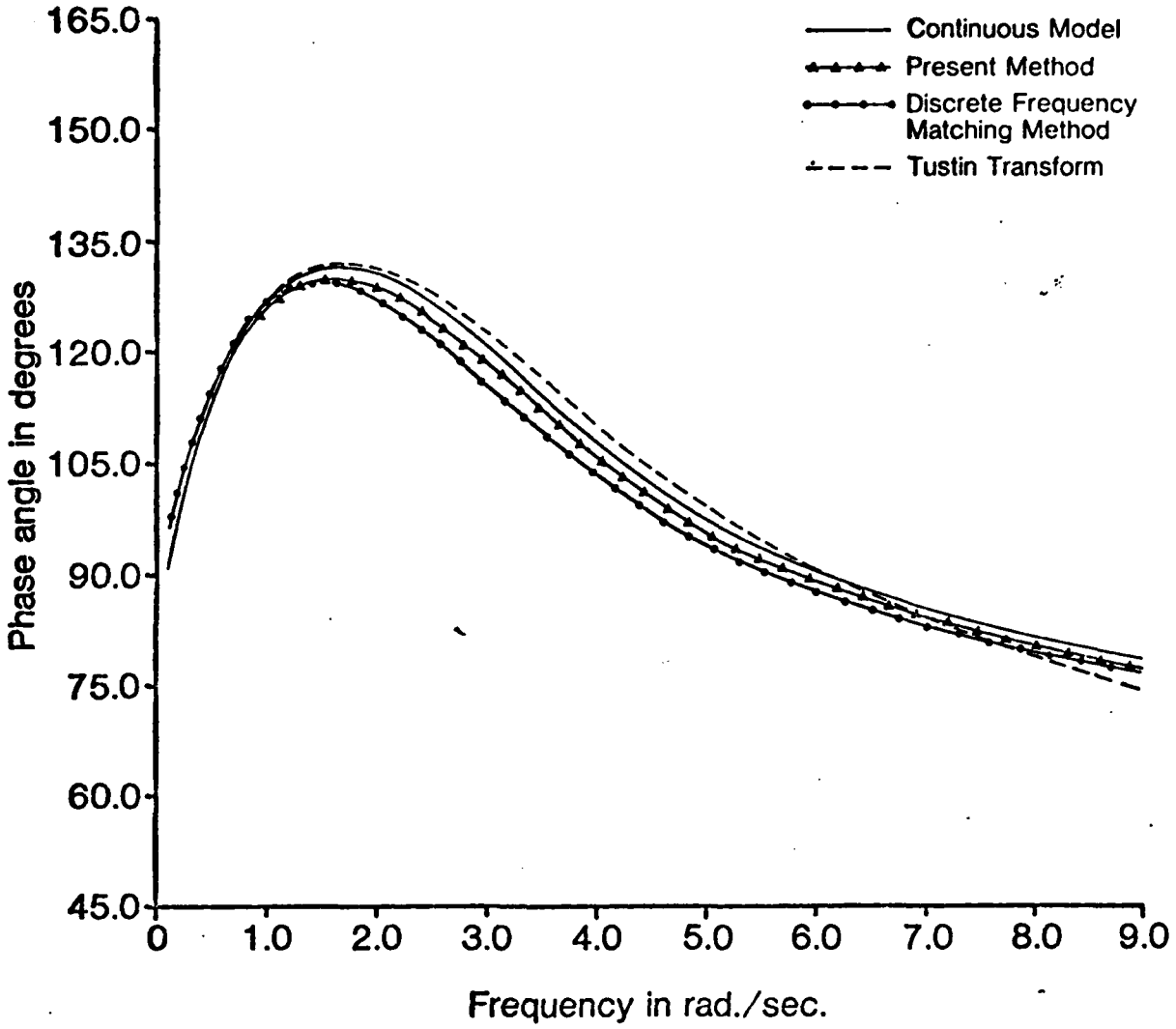

Figure 23. Phase plot of the frequency responses of the middle loop of the continuous system and the corresponding digital control system designed by different methods (example 2).

$D_4(z)$ Controller:

From Figure 13, the transfer function of the continuous model for the design of digital controller $D_4(z)$ can be written as

$$F_3(s) = \frac{a_n(s)}{R(s)} = \frac{F_2(s)G_3(s)}{1+G_{c4}(s)F_2(s)G_3(s)}$$

$$= -\frac{.649s^8+30.5s^7+559.9s^6+.5534\times10^4s^5+.3754\times10^5s^4+.1883\times10^6s^3}{s^9+62s^8+187.2s^7+.2359\times10^5s^6+.1711\times10^6s^5+.6447\times10^6s^4+.1373\times10^7s^3}$$

$$\frac{+.4981\times10^6s^2+.3417\times10^6s-627.1}{+.1021\times10^7s^2+.3466\times10^6s-332.3} \qquad (109)$$

In view of Figure 14 and equations (70) and (71), we can write

$$X_{11}+jY_{11} = \frac{j\gamma}{1+j\gamma\frac{T}{2}}\, z(j\gamma)\, \frac{s}{s+20}\, \frac{a_n(s)}{\delta e}\Bigg|_{s=j\frac{2}{T}\tan^{-1}\gamma\frac{T}{2}} \qquad (110)$$

and

$$X_{21}+jY_{21} = z(j\gamma)\frac{-.0076w^5-2.43w^4+138.8w^3+75.34w^2+.65w}{w^5+19.95w^4+15.74w^3-44.29w^2-.74w-.27}\Bigg|_{w=j\gamma} \qquad (111)$$

where

$$z(j\gamma) = \frac{D_2(w)}{1+\overline{G_{h0}G_1}(w)D_1(w)+\overline{G_{h0}G_1G_2}(w)D_2(w)D_3(w)}\Bigg|_{w=j\gamma} \qquad (112)$$

Loading equations (109)-(112) into the computer program written for the algorithm implementing equations (36)-(40), the pulse-transfer function of the digital controller $D_4(z)$ is given by

$$D_4(z) = 1.0124 \qquad (113)$$

The pulse-transfer functions of $D_4(z)$ obtained by the existing methods are given by

Tustin transform:

$$D_4(z) = \frac{.5858z^2+.10652-.479}{z^2-1.082+0.29} \tag{114}$$

Discrete frequency method:

$$D_4(z) = \frac{1.994z^2-3.716z+1.803}{z^2-1.8812z+.9577} \tag{115}$$

The frequency responses of the multi loop continuous system shown in Figure 13 and the digital control system shown in Figure 14 with digital controller $D_4(z)$ given by equations (113)-(115) are shown in Figures 24-26. Comparison of these results demonstrate the superiority of the present method over the existing methods.

SECTION V

CONCLUSIONS

A method for converting an existing multiloop continuous control system into a digital control system with similar performances is developed. An attempt is made to match the continuous frequency response of the digital control system as closely as possible with that of the continuous model. The parameters of the digital controllers are obtained by minimizing modified mean-square of the errors between the transfer functions of the continuous and the digital systems in the w-domain. Formulas for computing the parameters of the digital controllers are obtained and have been programmed for a computer. Since the design procedure is computer-aided, one may try out several digital controllers of different order and select the best design by considering the trade-off between the cost and performance.

The numerical examples considered show that the performance of the digital control system obtained by the method presented is superior to the ones obtained by the existing methods.

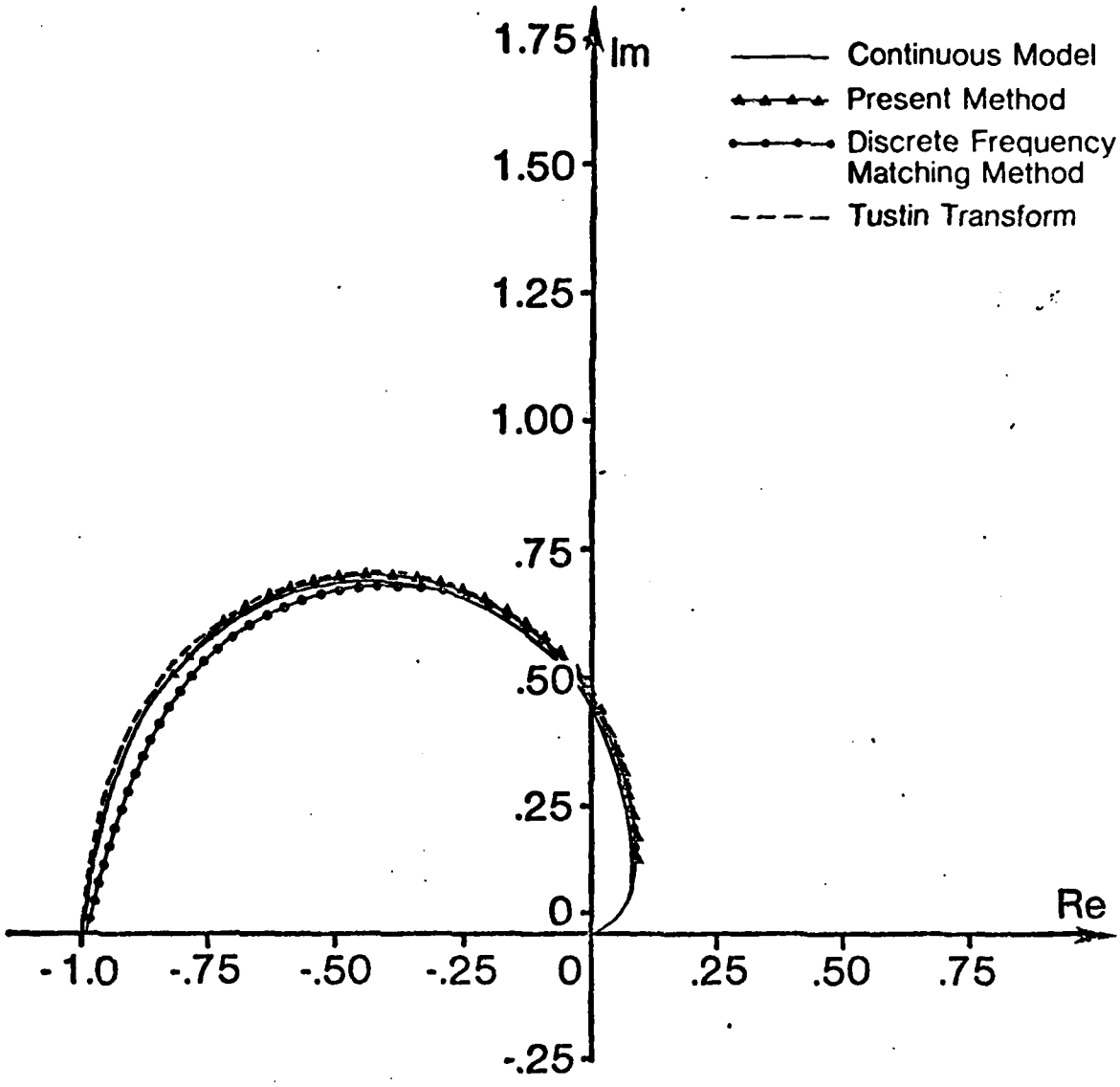

Figure 24. Nyquist plot of the frequency response of the multiloop continuous model and the digital control sytem designed by different methods (example 2).

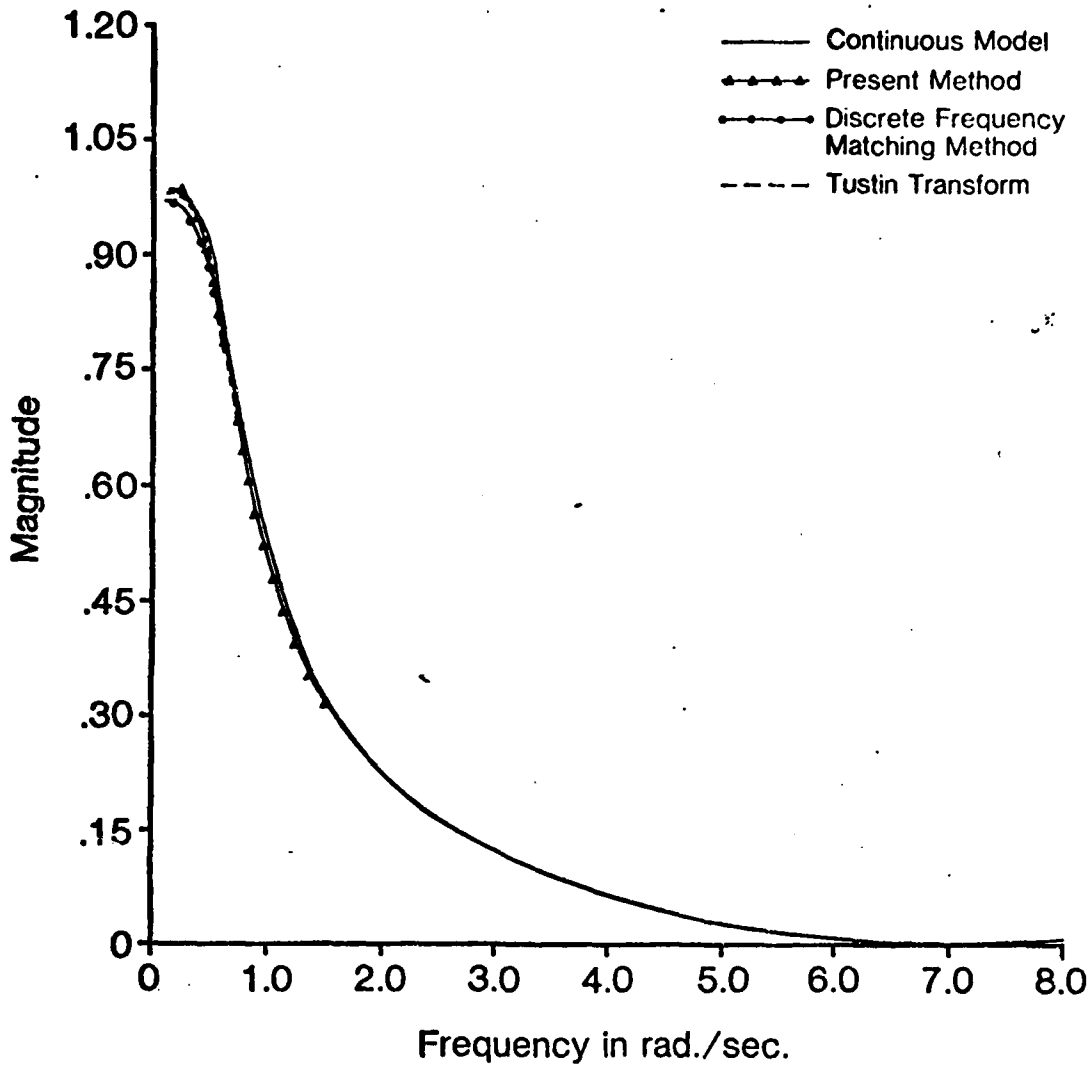

Figure 25. Magnitude plot of the frequency response of the multiloop continuous model and the digital control system designed by different methods (example 2).

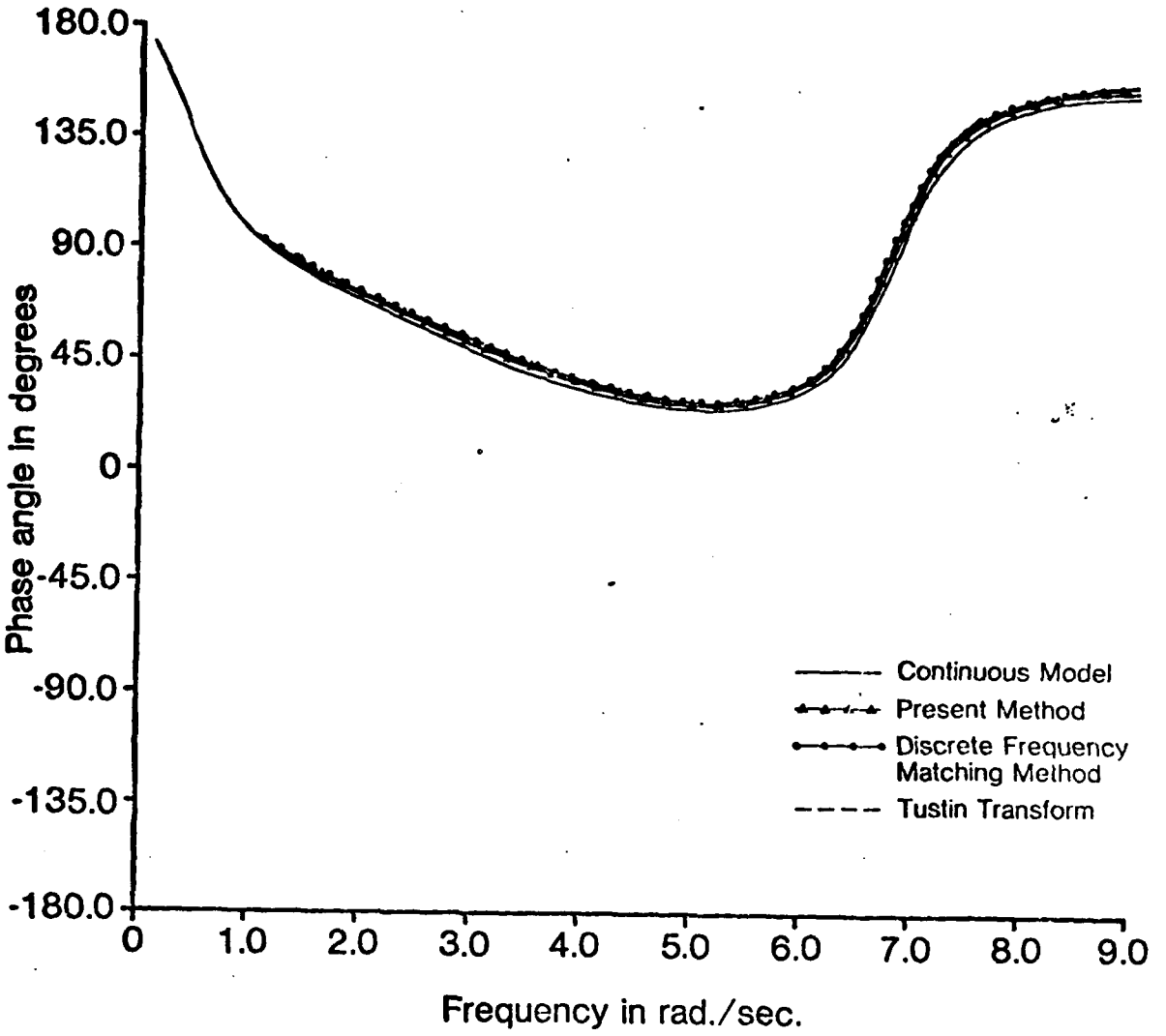

Figure 26. Phase plot of the frequency response of the multiloop continuous model and the digital control system designed by different methods (example 2).

APPENDIX A

LISTING OF TRANSFER FUNCTIONS

In this appendix, the transfer functions of the aircraft model (M = 0.6, h = 30,000 ft) used in Section IV are provided.

$\frac{20}{s+20}$ α/δ_e

NUMERATOR

I	NPOLY(I)	ZERO(I)
1	(-1.449)S** 3	(-.8003E-02) + J(-.7455E-01)
2	(-147.6)S** 2	(-.8003E-02) + J(.7455E-01)
3	(-2.370)S** 1	(-101.9) + J(0.)
4	(-.8295)	

DENOMINATOR

I	DPOLY(I)	POLE(I)
1	(1.000)S** 5	(1.137) + J(0.)
2	(20.95)S** 4	(-.9345E-02) + J(.7705E-01)
3	(16.71)S** 3	(-.9345E-02) + J(-.7705E-01)
4	(-46.66)S** 2	(-2.071) + J(0.)
5	(-.7820)S** 1	(-20.00) + J(0.)
6	(-.2837)	

$\frac{20}{s+20}$ q/δ_e

NUMERATOR

I	NPOLY(I)	ZERO(I)
1	(-147.6)S** 3	(0.) + J(0.)
2	(-79.39)S** 2	(-.8816E-02) + J(0.)
3	(-.6884)S** 1	(-.5292) + J(0.)
4	(0.)	

DENOMINATOR

I	DPOLY(I)	POLE
1	(1.000)S** 5	(1.137) + J(0.)
2	(20.95)S** 4	(-.9345E-02) + J(.7705E-01)
3	(16.71)S** 3	(-.9345E-02) + J(-.7705E-01)
4	(-46.66)S** 2	(-2.071) + J(0.)
5	(-.7820)S** 1	(-20.00) + J(0.)
6	(-.2837)	

$\frac{20}{s+20}$ $\frac{a_n/\delta_e}{}$

NUMERATOR

I	NPOLY(I)		ZERO(I)
1	(-.5315)S** 4	(0.) + J(	0.)
2	(-.5314)S** 3	(.1831E-02) + J(	0.)
3	(-24.95)S** 2	(-.5009) + J(	-6.833)
4	(.4567E-01)S** 1	(-.5009) + J(	6.833)
5	0.)		

DENOMINATOR

I	DPOLY(I)		POLE(I)
1	(1.000)S** 5	(1.137) + J(	0.)
2	(20.95)S** 4	(-.9345E-02) + J(	.7705E-01)
3	(16.71)S** 3	(-.9345E-02) + J(	-.7705E-01)
4	(-46.66)S** 2	(-2.071) + J(	0.)
5	(-.7820)S** 1	(-20.00) + J(	0.)
6	(-.2837)		

REFERENCES

1. D. Tabak, "Digitalization of Control Systems," Comput. Aided Des., Vol 3, No. 2, pp. 13-18, 1971.

2. B.C. Kuo, G. Singh and R.A. Yackel, "Digital Approximation of Continuous-Data Control Systems by Point-by-Point State Comparison," Comput. and Elect. Engng., Vol. 1, pp. 155-170, 1973.

3. R.A. Yackel, B.C. Kuo and G. Singh, "Digital Redesign of Continuous Systems by Matching of States at Multiple Sampling Periods," Automatica, Vol. 10, pp. 105-111,1974.

4. G. Singh, B.C. Kuo and R.A. Yackel, "Digital Approximation by Point-by-Point State Matching with Higher-Order Holds," International Journal of Control, Vol. 20, No. 1, pp. 81-90, 1974.

5. Kuldip S. Rattan and H.H. Yeh, "Digitalization of Control Systems." Computer-Aided Design. Vol. 3, No. 2, 13-18.

6. E.C. Levy, "Complex-Curve Fitting, "I.R.E. Trans. Automatic Control, Vol. AC-4, pp. 37-43, 1959.

7. Kuldip S. Rattan, "Digitalization of Existing Continuous-Data Control System," AFWAL-TM-80-105-FIGC.

8. G.J. Didaleusky and R.F. Whitback,"Multi-Rate Digital Control Systems With Simulation Applications," Vol. II, Technical Report AFWAL-TR-80-3101, Sep. 1980.

9. R.F. Whitbeck and L.G. Hofman, "Analysis of Digital Flight Control Systems with Flying Quality Applications," Vol. II, Technical Report AFFDL-TR-78-115, 1978.

10. R. Kalman, "Design of a Self-Optimizing Control System," Trans. ASME, Vol. 80, pp. 468-478, 1958.

11. S.V. Rao and S.S. Lamba, "A New Frequency Domain Technique For The Simplification of Linear Dynamic Systems," International Journal of Control, Vol. 20, No. 1, pp. 71-79, 1974.

12. Gene F. Ranklin and J. David Powell, Digital Control of Dynamic Systems, (Addison Wesley, 1980), p. 114.

13. R.F. Whitbeck and Dennis G.J. Didaleusky, "Multi-Rate Control Systems with Simulation Applications," Vol. I, Technical Report AFWAL-TR-80- 3101, May 1980.